



Page Proof Instructions and Queries

Please respond to and approve your proof through the “Edit” tab, using this PDF to review figure and table formatting and placement. This PDF can also be downloaded for your records. We strongly encourage you to provide any edits through the “Edit” tab, should you wish to provide corrections via PDF, please see the instructions below and email this PDF to your Production Editor.

Journal Title: Proceedings of the Institution of Mechanical Engineers, Part L: Journal of Materials: Design and Applications
Article Number: 1080115

Thank you for choosing to publish with us. This is your final opportunity to ensure your article will be accurate at publication. Please review your proof carefully and respond to the queries using the circled tools in the image below, which are available in Adobe Reader DC* by clicking **Tools** from the top menu, then clicking **Comment**.

Please use *only* the tools circled in the image, as edits via other tools/methods can be lost during file conversion. For comments, questions, or formatting requests, please use . Please do *not* use comment bubbles/sticky notes .



*If you do not see these tools, please ensure you have opened this file with **Adobe Reader DC**, available for free at get.adobe.com/reader or by going to Help > Check for Updates within other versions of Reader. For more detailed instructions, please see us.sagepub.com/ReaderXProofs.

No.	Query
GQ1	Please confirm that all author information, including names, affiliations, sequence, and contact details, is correct.
GQ2	Please review the entire document for typographical errors, mathematical errors, and any other necessary corrections; check headings, tables, and figures.
GQ3	Please confirm that the Funding and Conflict of Interest statements are accurate.
GQ4	Please ensure that you have obtained and enclosed all necessary permissions for the reproduction of artistic works, (e.g. illustrations, photographs, charts, maps, other visual material, etc.) not owned by yourself. Please refer to your publishing agreement for further information.
GQ5	Please note that this proof represents your final opportunity to review your article prior to publication, so please do send all of your changes now.
GQ6	Please note, only ORCID iDs validated prior to acceptance will be authorized for publication; we are unable to add or amend ORCID iDs at this stage.
AQ1	We have inserted Funding information from the metadata. Please check.
AQ2	Please provide page range in Ref. [4].
AQ3	Please provide the complete publication details (if missing) for all other-type references those are not having URL links

Influence of bone marrow characteristic and trabecular bone morphology on bone remodelling process with FSI approach

Proc IMechE Part L:
J Materials: Design and Applications
1–13
© IMechE 2022
Article reuse guidelines:
sagepub.com/journals-permissions
DOI: 10.1177/14644207221080115
journals.sagepub.com/home/pil



AAR Rabiatul¹, Devi Rianti^{2*}, SJ Fatihhi³, Amir Putra Md Saad⁴,
Zulfadzli Zakaria¹, Anita Yuliati³, MN Harun^{2,5}, MRA Kadir^{5,6},
Andreas Öchsner⁷ , Tunku Kamarul⁸, Khalid M Saqr⁹
and Ardiyansyah Syahrom^{1,2*} 

GQ1 = OK

GQ2 Abstract

GQ2 = OK

GQ4 While doing daily physiological activities, the trabecular bone will experience a certain amount of deformation which leads to the bone marrow movement. The movement can affect the bone remodelling process and the properties of the bone itself. The bone marrow plays a role as a hydraulic stiffening of the trabecular structure. However, previous studies analysed on trabecular bone and bone marrow separately, which is not considered as the actual condition. Thus, it is crucial to consider combine analyses of the bone marrow with the trabecular structure simultaneous. The aim of this study is to investigate the effect of bone marrow on the mechanical environment and the structure of trabecular bone during normal walking loading. Hence, this study used the Fluid-Structure Interaction (FSI) approach as a finite element method to discover the effect of bone marrow to the trabecular structure and vice versa. The findings show the shear stress value along normal walking phase was found in a range of 0.01–0.27 Pa which is sufficient to regulated cell response minimally. This study provides insight into understanding the related mechanobiological responds towards supply of nutrients onto bone cells.

GQ4 = All Artistic Work Originally by our work

Keywords

Fluid Structure Interaction, Trabecular Bone, Bone Marrow, Shear Stress, Stiffness, Bone Remodelling

Date received: 10 October 2021; final manuscript received January 27, 2022; accepted: 27 January 2022

Introduction

Physiological loading induced trabecular bone deformation that leads to the bone marrow movement within the porous structure which contribute to stimulating the osteogenic response to the bone cells.¹ The forces from the physiological loading cause both small strain and shear stress which known as a key to initiate the bone remodelling process.^{2–5} Currently, researchers tried to discover the actual value necessary to stimulate the bone cells for the bone remodelling process. To this date, experimental and simulation study have been performing in order to capture the value of these biomechanical stimuli that encourage the remodelling process.^{6–8} Bone marrow is a prime component in trabecular bone, in which it accommodates bone predecessors' cells for bone remodelling. Thus, it is important to consider its presence to better represent the actual conditions of trabecular bone. Therefore, knowledge of biomechanical environment that occur within the trabecular bone during daily physiological activities is necessary to comprehend on how the bone marrow can affect the bone remodelling.

Physiological loading includes daily activities such as house chores, daily walking, and sports activity helps in

¹Medical Device Technology Center (MEDiTEC), Institute Human Centred Engineering (iHumEn), Universiti Teknologi Malaysia, Johor, Malaysia

²Dental materials science Department, Faculty of Dentistry Medicine, Universitas Airlangga, Surabaya, Jawa Timur, Indonesia

³Universiti Kuala Lumpur, Malaysian Institute of Industrial Technology, Kuala Lumpur, Malaysia

⁴School of Mechanical Engineering, Faculty of Engineering, Universiti Teknologi Malaysia, Johor, Malaysia

⁵Sports Innovation and Technology Centre (SITC), Institute Human Centred Engineering (iHumEn), Universiti Teknologi Malaysia, Johor, Malaysia

⁶School of Biomedicals Engineering and Health Sciences, Faculty of Engineering, Universiti Teknologi Malaysia, Johor, Malaysia

⁷Lightweight Design / Structural Simulation, Faculty of Mechanical Engineering, Esslingen University of Applied Sciences, Esslingen, Germany

⁸Tissue Engineering Group (TEG), National Orthopaedic Centre of Excellence in Research and Learning (NOCERAL), Department of Orthopaedic Surgery, Faculty of Medicine, University of Malaya, Kuala Lumpur, Malaysia

⁹College of Engineering and Technology, Arab Academy for Science, Technology and Maritime Transport, Alexandria, Egypt

Corresponding author:

Ardiyansyah Syahrom, Medical Device Technology Center (MEDiTEC), Institute Human Centred Engineering (iHumEn), Universiti Teknologi Malaysia, Skudai, 81300, Malaysia.
Email: ardiyans@gmail.com

GQ5 = We have 2 Corresponding, Please add another one Please refer another box

Devi Rianti
Dental materials science Department, Faculty of
Dentistry Medicine, Universitas Airlangga
Surabaya, Jawa Timur, Indonesia
devi-r@fkg.unair.ac.id

maintaining the bone health by transferring force to the bone structure. These can be seen on immobilization and bedrest individual that had reduce in their bone mass.^{9,10} These relationship of loading and bone formation had been support with the Wolff's law since 1892.¹¹ The trabecular bone experience compression and tension in the microstructure due to the loading causing the micro strain which one of the mechanical stimuli. Previous study reported that the physiological activities initiate in range of 0.001–0.003 mm/mm on the trabecular structure.^{12,13} However, minimal physiological activity cause 1000 μe which cause bone resorption process higher compare to the bone resorption.¹⁴ Amazingly the bone can heal itself when there is external loads act upon the cells which can help in cells excite by signalling to the bones to start building themselves up. Then again, the loads from human daily life will also initiate the movement of bone marrow within the structure which cause the shear stress that act as response to the remodelling process.¹⁵

The osteogenic response include osteoprogenitor cells secrete autocrine factors, for example prostaglandins E_2 (PGE_2) and nitric oxide (NO), which can regulate the remodelling activity.¹⁶ In addition, the proliferation rates have been found increasing when the bone marrow stromal cells were exposed to the fluid flow, which means higher number of cells participate in bone formation.¹⁷ The mesenchymal stem cells (MSCs) has been actively investigate in experiment and simulation due to its ability to differentiate into other cells such as osteoblast (bone cells), chondrocytes (cartilage cells) and adipocytes (fat cells).^{18–20} The shear stress known as one of the parameters required for the MSCs in the bone marrow to differentiate and assists the remodelling activity.^{20,21} The range of shear stress need for the cells to response mention by previous study is about 0.02 to 1.0 Pa.^{2,22–25} Undoubtedly, bone remodelling process also requires adequate nutrient transport through the bone cells. These were also with help of bone marrow which function to transport the nutrient and remove waste. However, knowledge on how shear stress value contributing in MSCs to differentiate to different cells are still shallow.

In the present work the movement of the bone marrow regulate osteogenic responds which relate to the trabecular bone deformation due to the physiological activity. Thus far, there is no study using physiological gait loading as boundary to examine the effect of interaction on mechanical stimulus and trabecular bone. Therefore, the aim of this study is to investigate the effect of bone marrow mechanical environment and trabecular bone structure during normal walking loading. A fluid structure interaction (FSI) approach was applied to determine the deformation of trabecular bone with corresponding of marrow shear stress in bone remodelling activity.

Materials and methods

Sample preparation

The fresh bovine femur bones were harvested from the local slaughterhouse and kept frozen at -18°C to 26°C .

Specimens of trabecular bone were taken by using a Bosch circular saw with copious water irrigation. The femur bone was then divided and cut into a section of medial condyle, femoral neck and femoral ball with the vertical orientation due to the maximum extension of knee joint occurred. The trabecular bone was then again cut into a cubic shape ($10\text{mm} \times 10\text{mm} \times 17\text{mm}$) in length by using a precision cutting tool (Allied Techcut, USA). The precision cutter consists of diamond-resin bonded wafering blade with a minimum speed of 150–250 rpm with continuously water irrigation to prevent heat-related damages. Then, the specimens were placed in small airtight plastic bag with the purpose of reducing the thermal cycling and stored in the freezer with a temperature below -26°C . After that, the specimens will go through next procedure using the ultrasonic cleaner (Crest ultrasonic, model P11000SR, USA) additional with a chemical detergent (Pumicedcitrius, Gent-I-kleen, USA) to cleaned from marrow. The specimens were then submerged for about 10–15 min at a temperature below 46°C . In order to remove the loose particles and excessive marrow, the specimens were then air-jetted and vacuumed suction. This procedure was repeated until all excessive marrow is removed (Fatihhi SJ et al. 2015). A custom jig was used to align the specimen for improved vertical oriented. Afterwards, the specimens sealed in an airtight bag placed in a -20°C freezer and frozen overnight while the adhesive completely cured. Only then, the samples are scan by using the $\mu\text{-CT}$ scanner (SkyScan 1172, Bruker MicroCT, Belgium).

Model development

The two-dimensional image data sets from the $\mu\text{-CT}$ scan were stacked in sequence by Mimics software (MIMICS 12, Materialise, Belgium) and converted into rectangular shape to construct the trabecular model. The thickness of each images slice is $15\ \mu\text{m}$. The stacked image datasets were calculated into three-dimensional trabecular model through image segmentation by the Mimics software. Subsequently, the image datasets were thresholded to select the region of interest for three-dimensional constructed model. In addition, by using an adapted marching cubes algorithm, the triangular surface meshes were generated for the trabecular model. Then again, the result of triangular surface mesh was very fine, which needed to follow with step of removing noise, redundant parts and irregularities shape to construct accurate three-dimensional models. There were 10 models generated and tested in this study.

As for finite element analysis simulation, small sized sub volume region of interest was selected from the fine mesh trabecular bone constructed models (Figure 1) due to the limitation of computer capability to complete the simulation study. These models were then converted into finite element mesh for the simulation. In addition, the trabecular bone model surface meshes with jagged or bad sector are also repaired before importing the

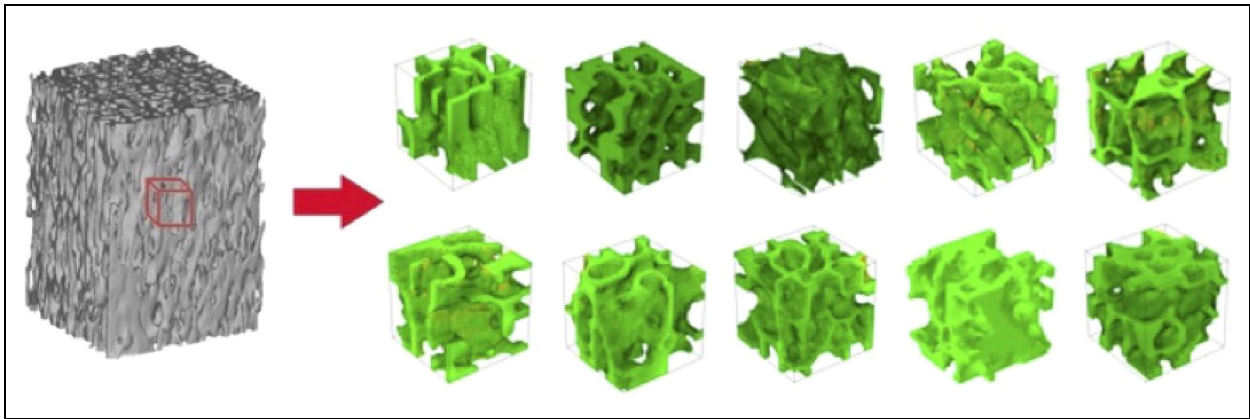


Figure 1. Development of three-dimensional model into sub volume model.

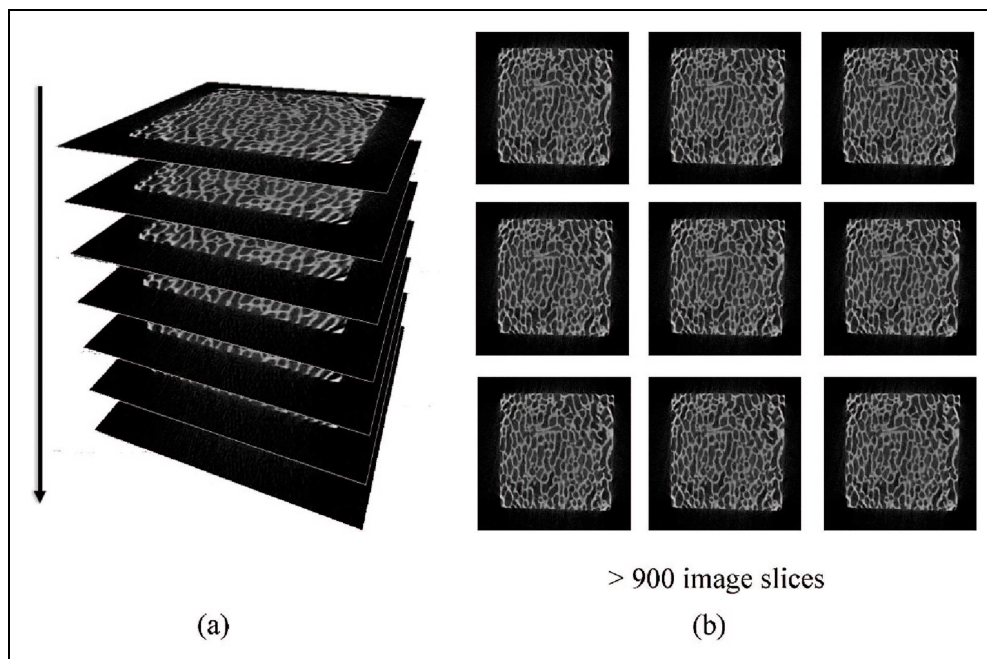


Figure 2. Images obtain from μ -CT scan with (a) images stacked in sequence according to sample orientation (b) raw scanned images file.

model. For the FSI study purpose, the outer wall of the models needed to convert into a flat surface. Thus, for the model preparation, the smaller size sub-models were then merged with cube surface mesh in the Mimics software. After that, the uneven surface of trabecular sub volume models was removed according to the sub volume model shape. Then, the space between the sub model and the cube were stitch together by creating a triangular mesh in between the space. These steps were applied to all six surfaces for the sub trabecular model. Finally, the surface mesh is exported to an STL format file.

Morphology study. From the μ -CT scan images, the morphological study was conducted. One of a trabecular bone sample contains approximately 900 image slices (Figure 2 (b)). The morphological indices were measured

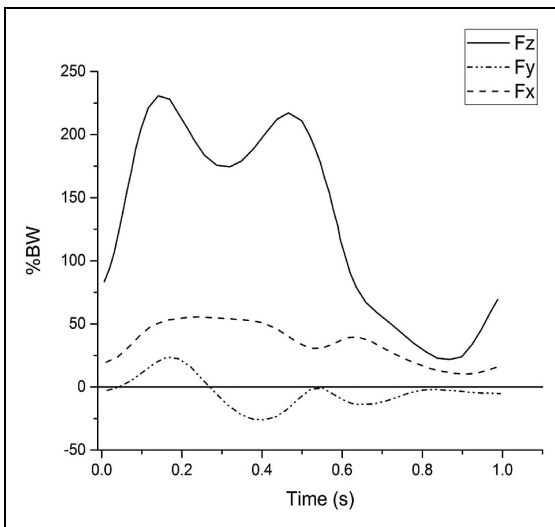
using ImageJ (ImageJ, National Institute of Health, USA). All these slices were import and stacked (Figure 2 (a)) by using BoneJ plugins in ImageJ software to obtain the trabecular morphological data. The parameters measured included BV/TV, Tb.Th, Tb.Sp, Tb.N, DA, MIL, etc. All data present in Table 1.

Computational simulation

Two-way fluid-structure analysis were conducted using COMSOL Multiphysics software with purpose of investigate the fluid behaviour of bone marrow under gait loading conditions. A gait loading which representing normal walking were applied through the cap faces feature which considered as a rigid body. The gait loading (Figure 3) applied in multi-axis according to normal walking phase.²⁶ The normal walking phase of

Table 1. Morphological indices of trabecular bone sample.

Parameter	Minimum	Maximum	Mean	SD
BV/TV	0.318	0.477	0.379	0.057
Tb.Th (mm)	0.128	0.559	0.207	0.057
Tb.Sp (mm)	0.253	1.022	0.441	0.137
BS/BV	11.313	15.857	13.677	1.719
DA	0.38	0.684	0.611	0.146
Conn.D (mm ⁻³)	19.625	59.875	37.975	14.179
SMI	0.875	1.918	1.416	0.316
Porosity (%)	62	76	70	5
Bone Surface Area (mm ²)	28.802	37.518	32.447	3.134

**Figure 3.** Gait loading of normal walking based on body weight percentage (bergmann G. et al., 2001).

gait cycle was divided into 40 discrete points for the simulation. The cap faces feature is vital in the FSI study due to restriction coupling between the trabecular model and marrow model within the FEA. In addition, the prescribed displacement was applied to the cap, where the domain was restricted in the X and Y directions (Figure 4). As for the fluid boundary, the plane of the bottom boundary of fluid was applied as symmetry in order to ensure that the marrow volume remains within the domain when there is load applied through the structure. Moreover, in order to prevent normal velocity to the respective boundary, the marrow flow was model as symmetric in their normal directions. The convergence analysis in this study conclude that 400 thousand tetrahedral elements and shape function was used tessellation method is Delaunay on average were needed for accurate result computation (see Figure 5). In addition, the FSI interface uses an arbitrary Lagrangian-Eulerian (ALE) method, which allows moving boundaries without the need for the mesh movement to follow the material. This ALE method combined the fluid flow formulated using a Eulerian description and a spatial frame with solid mechanics formulated using a Lagrangian description and a material frame. The analysis was performed with the criterion of the von Mises stress criterion less than 5%.

The time-dependent solution is obtained for every gait cycle. Details on the force parameters implemented in this study was demonstrated in.²⁷ The solid trabecular structures were modelled as a linear elastic material.²⁸ An elastic modulus (E) of 1000 MPa²⁹ and Poisson's ratio of 0.3 was attributed to the trabecular bone solid structure.³⁰ Additionally, the viscosity of fluid marrow was assigned 0.4 Pa.s and modelled as incompressible according to Bryant et al.³¹ Newtonian fluid with density of 1060 kg/m³.³² The surface between the trabecular structure and marrow fluid is assigned as no-slip boundary.

In the present work, the bone marrow was modelled as an incompressible liquid. The incompressible Navier-Stokes equation was considered as the governing equation, in which;

$$\nabla \cdot u_{fluid} = 0 \quad (1)$$

On the other hand, the momentum equation was as follows;

$$\rho \frac{\partial u_{fluid}}{\partial t} + \rho(u_{fluid} \cdot \nabla)u_{fluid} = \nabla \cdot [-pI + \mu(\nabla u_{fluid} + (\nabla u_{fluid})^T)] + F \quad (2)$$

where the external force acting on the fluid was denoted by F , and gravity was neglected. Meanwhile, equation for solid at local equilibrium is given by;

$$\rho \frac{\partial^2 u_{solid}}{\partial t^2} - \nabla \cdot \sigma = F_v \quad (3)$$

where σ and F_v are the Cauchy stress tensor and body force, respectively. Deformed structure was demonstrated by u_{solid} , whereas the Piola-Kirchhoff stress, S was used to calculate the Cauchy stress using the following equation;

$$\sigma = J^{-1} FSF^T. \quad (4)$$

Using the gradient of displacement vector u_{solid} , the deformation gradient, F can be expressed as;

$$F = (I + \nabla u_{solid}). \quad (5)$$

In which the identity matrix was denoted by I , and the Jacobian of the deformation is defined as;

$$J = \det(F). \quad (6)$$

Fluid domain was solved based on Eulerian formulation, while solid domain was solved based on Lagrangian

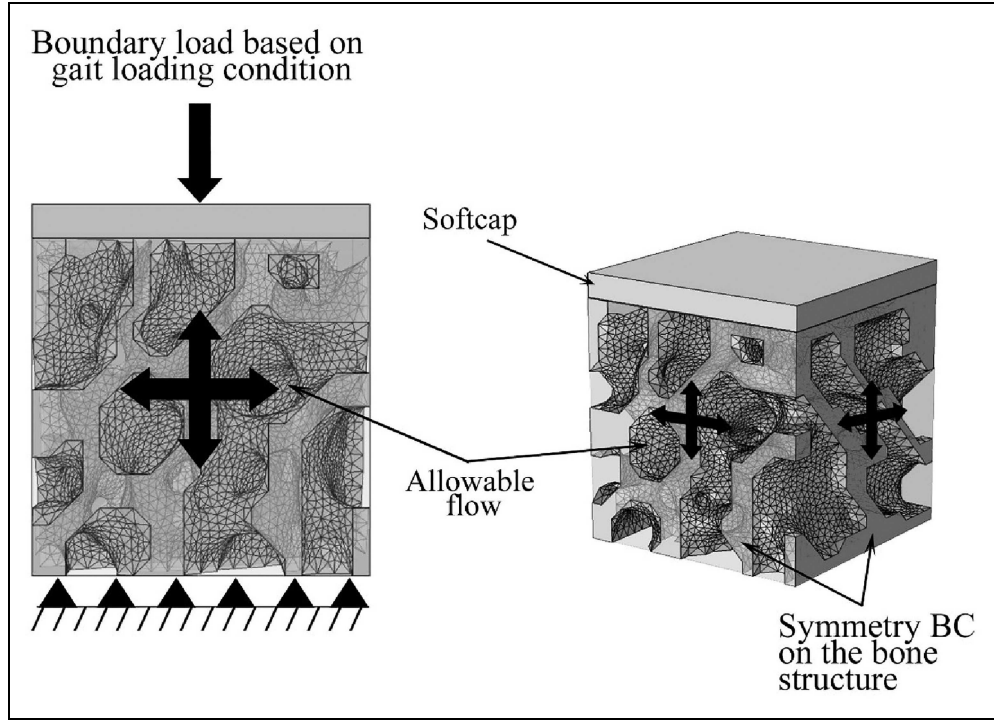


Figure 4. Boundary conditions (BC) of trabecular bone and bone marrow models.

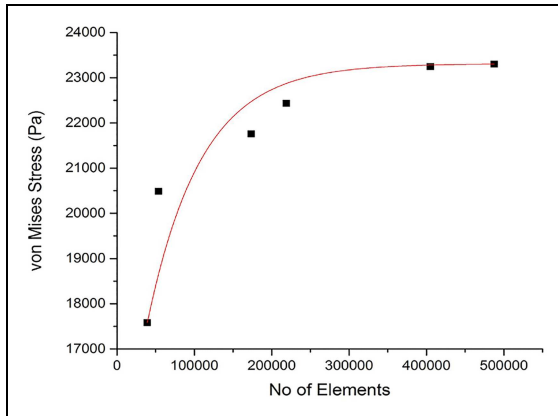


Figure 5. Convergence study for the trabecular structure model.

formulations. In coupling fluid-solid system, the arbitrary Lagrangian-Eulerian method can be implemented with total force on the fluid-solid boundary was given as;

$$f_r = n \cdot [-pI + \mu(\nabla u_{fluid} + (\nabla u_{fluid})^T)], \quad (7)$$

With \mathbf{n} is the normal acting outward at the boundary, the force at the structure's boundary is given by;

$$F_r = \sigma \cdot n. \quad (8)$$

In Spatial and material coordinate system, these forces can be coupled thru a force transformation using the arbitrary Eulerian-Lagrangian method as follows:

$$F_r = f_r \cdot \frac{dv}{dV}. \quad (10)$$

Mesh element scale factors dv and dV are the fluid and material frames, respectively. Further, the relationship of structural velocity of the moving wall with the fluid velocity is demonstrated as follows:

$$u_{fluid} = u_w, \quad (11)$$

Thus, the rate of change of the solid displacement is defined by the structural velocity.

$$u_w = \frac{\partial u_{solid}}{\partial t} \quad (12)$$

Statistical analysis

All morphology indices are presented in mean and standard deviation (Table 1). The Pearson's correlation and linear regression analysis were performed to explore the interrelationship between the morphological indices and the mechanical properties of the trabecular bone sample. The multiple linear regression was performed using IBM SPSS Statistics 23 (IBM Corp, USA). For all comparison, the level of significant for p-value was <0.05 .

Results

The average von Mises stress distribution during normal walking with cycle duration was plotted as shown in Figure 6. The peak pressure reached as high as 11.35×10^5 Pa. Then again, the minimum stress for trabecular bone is 10.75×10^4 Pa at period of 0.86s. As can be seen, the behaviour of von Mises stress during gait cycle is similar to the force in the vertical direction.

From the computational FSI simulation, the von Mises stress distribution within the trabecular bone model along gait normal walking gait loading cycle at different time frame as illustrated in Figure 7. Comparing Figure 7(a) and (b), more area covered with high stresses at time 0.14 s. These results match with the graph of the von Mises stress over time.

The pressure and shear stress distribution during gait loading cycle are presented in Figure 8. This figure shows how the structure of trabecular bone affects the fluid characteristic during the gait loading cycle. It can be observed from the Figure 8 that the pattern of pressure distribution was similar to the von Mises stress results. The pressure was range from 380 to 4070 Pa during the normal walking cycle. Moreover, as discussed earlier, the trabecular structure experience shear stress

due to bone marrow movement. With an average of 0.09 Pa, the shear stress was in the range of 0.01 to 0.27 Pa.

Based on 2D images of the trabecular model cross section, the pressure on top section was lower than below section when the structure at the highest compression deformation Figure 9(a). However, at period 0.86 s, the pressure on top section becomes higher than the lower section. Figure 10 shows velocity profile of marrow during gait loading cycle at different time frame. As can be seen, at period 0.14s, the velocity was higher than at period 0.86 s. The velocity was range of 0.09 $\mu\text{m/s}$ to 81.2 $\mu\text{m/s}$ at period of 0.14 s and 0.001 $\mu\text{m/s}$ to 2.6 $\mu\text{m/s}$ at period 0.86 s.

Multiple regression analysis for morphological parameters is tabulated in Table 2 and Table 3 with Pearson correlation and *p*-value for solid and fluid characteristic. Bone volume fraction and SMI shows good correlation

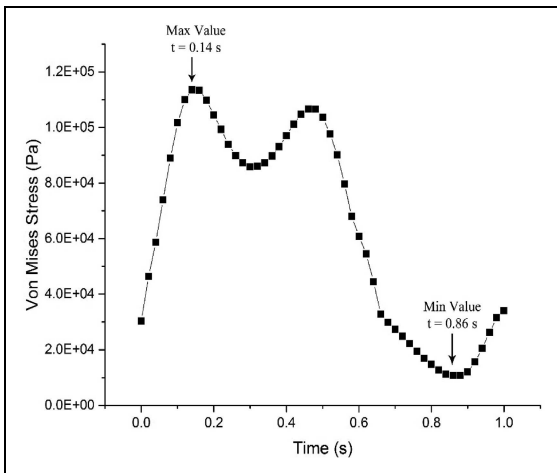


Figure 6. Von Mises stress distribution on the trabecular bone during normal walking.

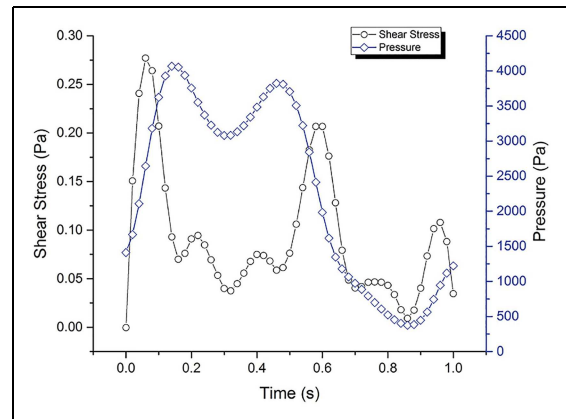


Figure 8. Maximum shear stress and pressure distribution on the trabecular bone along with normal walking loading.

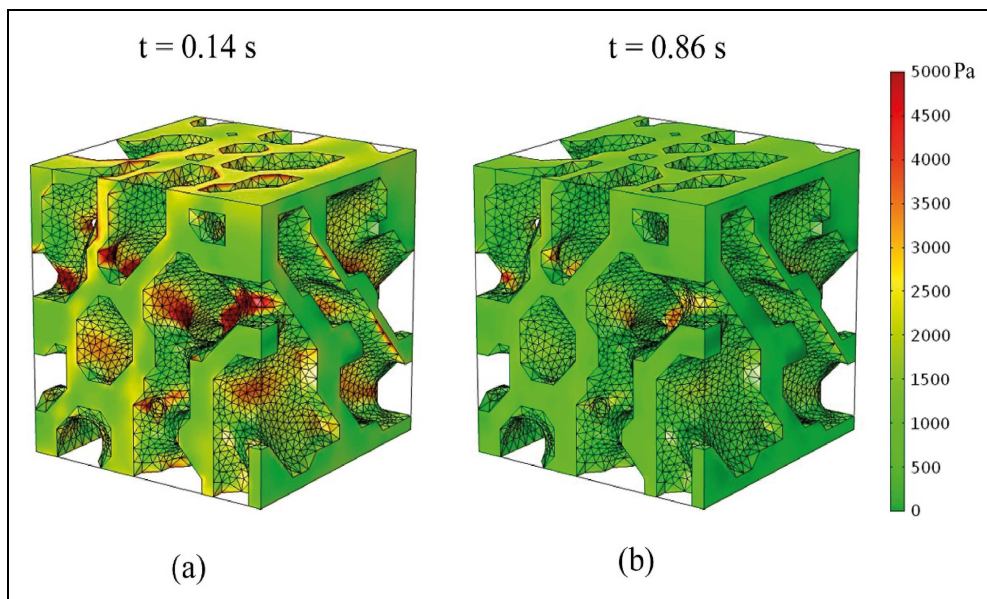


Figure 7. Comparison of von Mises stress on the trabecular bone at different time frame (a) $t = 0.14$ s and (b) $t = 0.86$ s.

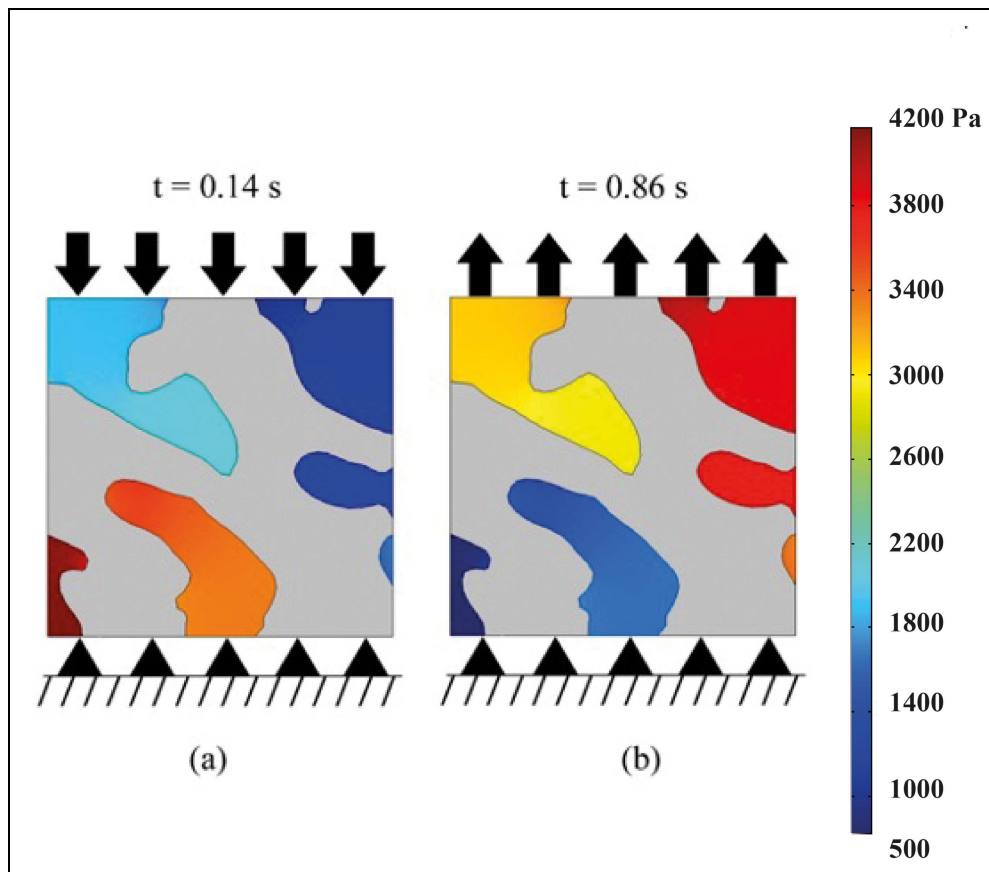


Figure 9. Comparison of pressure distribution on the trabecular bone cross section at different time frame (a) $t=0.14$ s and (b) $t=0.86$ s.

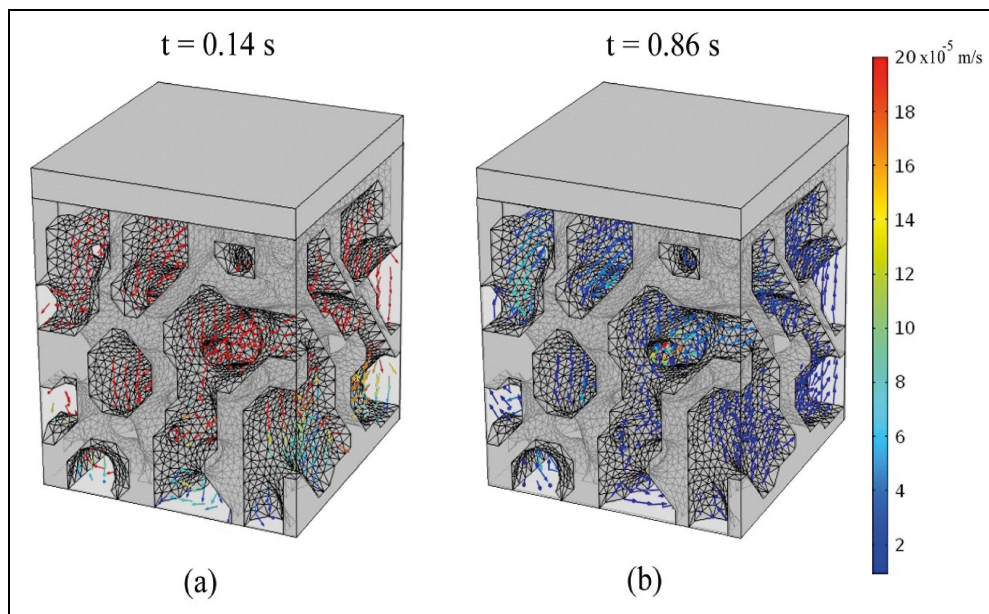


Figure 10. Velocity profile on the trabecular bone at different time frame (a) $t=0.14$ s and (b) $t=0.86$ s during normal gait loading.

with principal strain and von Mises stress. However, the SMI value only significant with principal strain and bone volume fraction solitary shows significant value with von Mises stress. As for marrow characteristic, velocity and

pressure were significant to SMI, while shear stress is insignificant with all morphological parameters.

The volume fraction plays a major role in trabecular bone mechanical properties. The distribution of von

Mises stress on different model with different bone volume fraction is shown in Figure 11. As can be seen, low bone volume fraction model result in higher von Mises stress compare with a model which has high volume fraction.

The permeability and trabecular stiffness relationship to bone volume fraction and SMI are plotted in Figure 12. The graph showed a strong and negative correlation between the permeability and bone volume fraction ($r = -0.862$), whereas the correlations are strong and positive between permeability and SMI ($r = 0.835$). Meanwhile, in Figure 13 shows both bone volume fraction and SMI have a strong correlation with the trabecular stiffness ($r = 0.832$ and $r = -0.796$; respectively). However, the trabecular bone stiffness correlation was inversely compared to the permeability.

Discussion

The trabecular bone structure is known as a porous structure which contributes to maximum strength while giving the bone less weight. Understanding the bone marrow flow and trabecular bone structure mechanism can provide insight into bone remodelling process and bone strength. It is vital to identify which architectural features

Table 2. Morphological parameters of trabecular bone sample with Pearson correlation and p-value in relation with mechanical behaviour.

Morphological Parameters	Principle Strain		Von Mises Stress	
	Pearson Correlation	p-value	Pearson Correlation	p-value
BV/TV	-0.830	0.123	-0.798	0.006*
BS/TV	0.449	0.452	0.28	0.132
SMI	0.850	0.002*	0.715	0.689
Conn. D	-0.032	0.916	-0.303	0.16
Tb.Th	-0.426	0.566	-0.344	0.206
Tb.Sp	0.705	0.403	0.769	0.405
DA	0.410	0.966	0.559	0.218

*Significant p-value < 0.05.

that affect the trabecular strength. Thus, in this study, finite element analysis with FSI approach was used to identify the architecture contribution with the presence of bone marrow when there is physical loading involved.

During physiological activities, the bone will have a deformation due to the mechanical load.³ The compressive and tensile stress is generated in the trabecular structure which causes the bone marrow within the structure to drift from region of compression to tension. Due to the complex structure of trabecular bone with small rods, plated and pores, there will be shear stress generated on the wall structure. Bone marrow function in activating the bone cells to start the bone remodelling process. Thus, this study analysed shear stress, pressure, and permeability to identify the fluid characteristic through physical activity. Moreover, the trabecular bone architecture and volume fraction play an important role in its mechanical properties. In addition, this study analysed the bone marrow permeability and trabecular stiffness with correlation to the trabecular morphology. Applied physiological gait loading in this present study to assure more reliable and safer prediction of bone marrow behaviour and trabecular stiffness.

In the analysis, it can be seen that the maximum peak von Mises stress range for all ten models are 91 kN/m² to 114 kN/m². The maximum value was identified in period 0.14s, which is due to the fact that higher contact force occurs at that period of time (Figure 7). Assessing the von Mises stress in the trabecular model was necessary with purpose of providing new insight in prediction of trabecular structure failure and evaluating the fracture risk. The permeability in this study was also in agreement with results from the literature.

The aim of this study is to identify the bone marrow movement behaviour within the trabecular structure sufficient for bone cell growth based on physiological activity. Normal walking loading was chosen since it is reported as the most frequent physiological activity.²⁶ The results show that during normal walking loading, the maximum shear stress occurs is all models are in range 0.05 Pa to 0.27 Pa. Furthermore, Li et al.¹⁷ Castillo and Jacobs²⁰ present that the shear stress was needed for the cells to differentiate and proliferate. Moreover, the previous

Table 3. Morphological parameters of trabecular bone sample with Pearson correlation and p-value in relation with fluid characteristics.

Morphology Parameters	Velocity		Pressure		Shear Stress	
	Pearson Correlation	p-value	Pearson Correlation	p-value	Pearson Correlation	p-value
BV/TV	-0.661	0.969	-0.672	0.168	0.001	0.499
BS/TV	0.388	0.449	0.53	0.585	0.411	0.119
SMI	0.710	0.022*	0.825	0.003*	0.029	0.469
Conn. D	-0.049	0.316	0.288	0.815	0.184	0.306
Tb.Th	-0.296	0.395	-0.346	0.209	-0.424	0.111
Tb.Sp	0.607	0.735	0.594	0.754	-0.255	0.239
DA	0.324	0.468	0.074	0.721	0.079	0.414

*Significant p-value < 0.05.

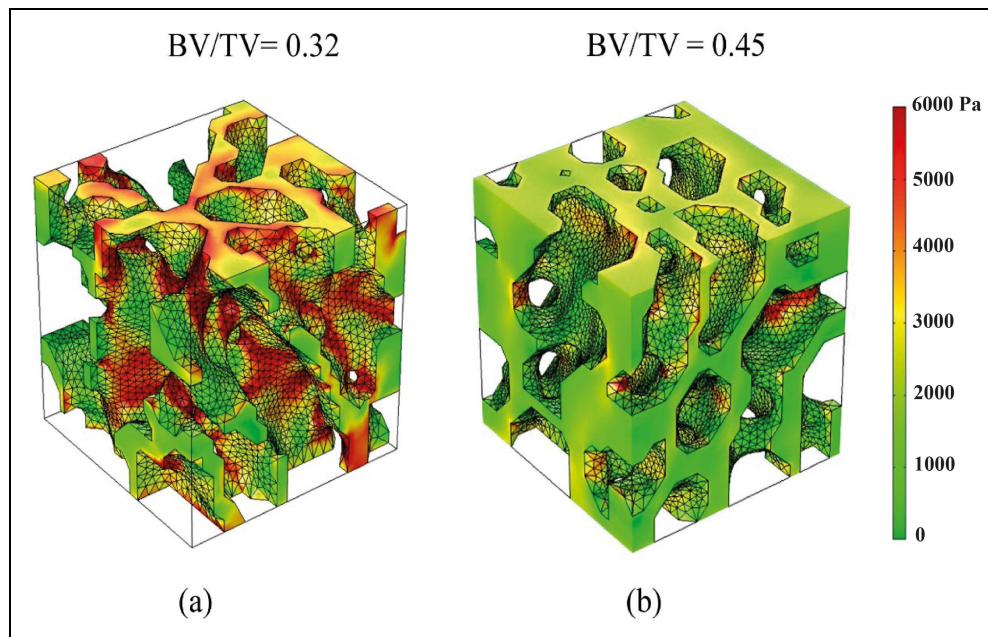


Figure 11. Comparison of von Mises stress on the trabecular bone with different bone fraction (a) $BV/TV = 0.32$ and (b) $BV/TV = 0.45$.

experimental study showed that shear stress in the range of 0.1 Pa to 1 Pa needed to stimulate bone cells in vitro. Thus, a much lower range of shear stress is suggested to simulate the stress on bone cells during normal walking. However, other previously study mention that 0.23 Pa of shear stress is sufficient for regulated bone cells to respond and synthesise bone matrix protein for bone remodelling process.³³ Additionally, there is separate study by Nauman et al.³⁴ stated that the bone cells stimulation is unaffected by difference shear stress levels.

Walking 10000 step per day has been proposed as daily activity for healthy adults. This recommendation was studied, and it is found that 10000 step per day can improve individual's health and sustainability. For example, previous studies stated higher step count per day could lower the prevalence of depression.³⁵ In addition, it is observed the Body Mass Index (BMI) of the group with higher step count per day has shown significantly lower compared with another group.³⁶ Nevertheless, there is no studies indicate on bone health based on daily step count. However, based on the results of this study, it is suggested that higher step count will lead to more shear stress. Thus, can help in improving the bone remodelling process and bone strength.

Moreover, while the trabecular bone deforms according to the physiological load, there would be pressure difference within the structure (Figure 8). Previous study stated bone formation increase with pressure. Welch et al.³⁷ in their study found that bone marrow pressure increased about 2000 Pa resulted in bone remodelling. Another study on the new bone formation of mouse tibiae, stated in dynamic compression induced a similar range of pressure value.³⁸ This study results for pressure

distribution in normal walking gait loading for all models was in the range of 180 Pa to 4000 Pa. Addition to this study result analysis, it is found that higher bone volume fraction will lead to lower pressure value (Table 3). However, the pressure difference also depends on a variety of factors, including the bone marrow rheology, bone strain and permeability.^{39,40}

In addition, the results show that the pressure gradient along the walking gait loading was different at period 0.14s and 0.86 s as in Figure 9. This is where the bone marrow function as hydraulic stiffening effect. Hydraulic stiffening effect refers to the reduction of bone stress during dynamic loading effect by the presence of fluid within the structure.⁴¹ While at period 0.14s is when the maximum compression occurs, the pressure of bone marrow was high at the bottom. This pressure might support a certain amount of applied load which caused the apparent stiffness to the trabecular structure. Similarly, at period of 0.86s, where tensile occur, the pressure was high at the upper region giving the structure extra load barrier which prevents the structure to have high deformation.

This study used BoneJ plugin in the ImageJ software to analyse the morphological data of the trabecular model. In the correlation study, only bone volume fraction (BV/TV) and SMI shows a significant value with the simulation results. Thus, this study correlated the permeability and bone stiffness with these both morphological parameters. From the results, permeability and stiffness show good correlation with the BV/TV. Permeability in trabecular bone was vital since it demonstrated the biological based features of trabecular bone. Still, the simulation results were consistent to those found in the previous literature.⁴² Additionally, the trabecular bone mechanical

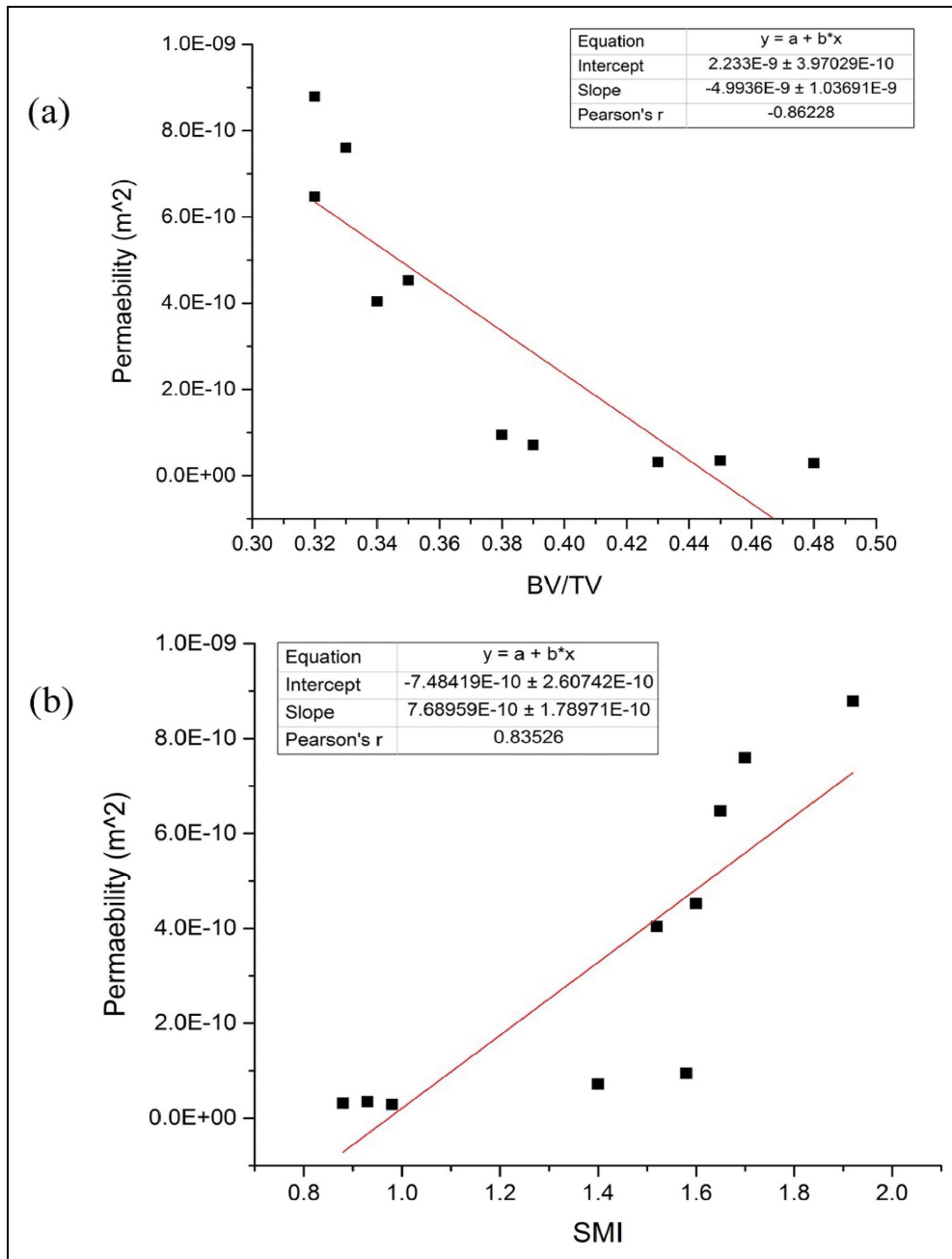


Figure 12. Linear relationship between (a) BV/TV and (b) SMI with permeability.

quality was depending on its stiffness, since the stiffness have a strong correlation with the strength.⁴³

Hypothetically bone with lower bone volume fraction means porous structure (osteoporotic bone). Thus, as mention by Goldstein et al.⁴⁴ and Syahrom et al.⁴⁵ the trabecular bone integrity and bone marrow permeability can be disarrange based on the porosity value. In addition, the results of this study suggests that enhancement of bone remodelling process can be achieved by optimization of BV/TV and permeability value. However, from the results analysis the reduction of BV/TV can cause higher stress on the trabecular structure (Figure 11) and the loss of trabecular structure stiffening effect (Figure 13). Therefore, important to find the optimum bone volume

fraction which has a good stiffening value and yet able to deliver sufficient nutrient to bone cells.

Other than bone volume fraction, the SMI also shows high correlation with the stiffness. The SMI is a measurement which determines a porous structure is made of rod or plate-like structure. The value starts from 0 for ideal plate structures to 3 for ideal rod structure.⁴⁶ Theoretically, the plate-like structure could barricade more fluid flow compared to the rod-like structure. In contrast with the permeability, the stiffness is negatively correlated with the SMI. Moreover, previous study already stated that trabecular plates have more dominant role in mechanical integrity of trabecular bone structure.^{47,48} Also, osteoporotic trabecular bone has been found to

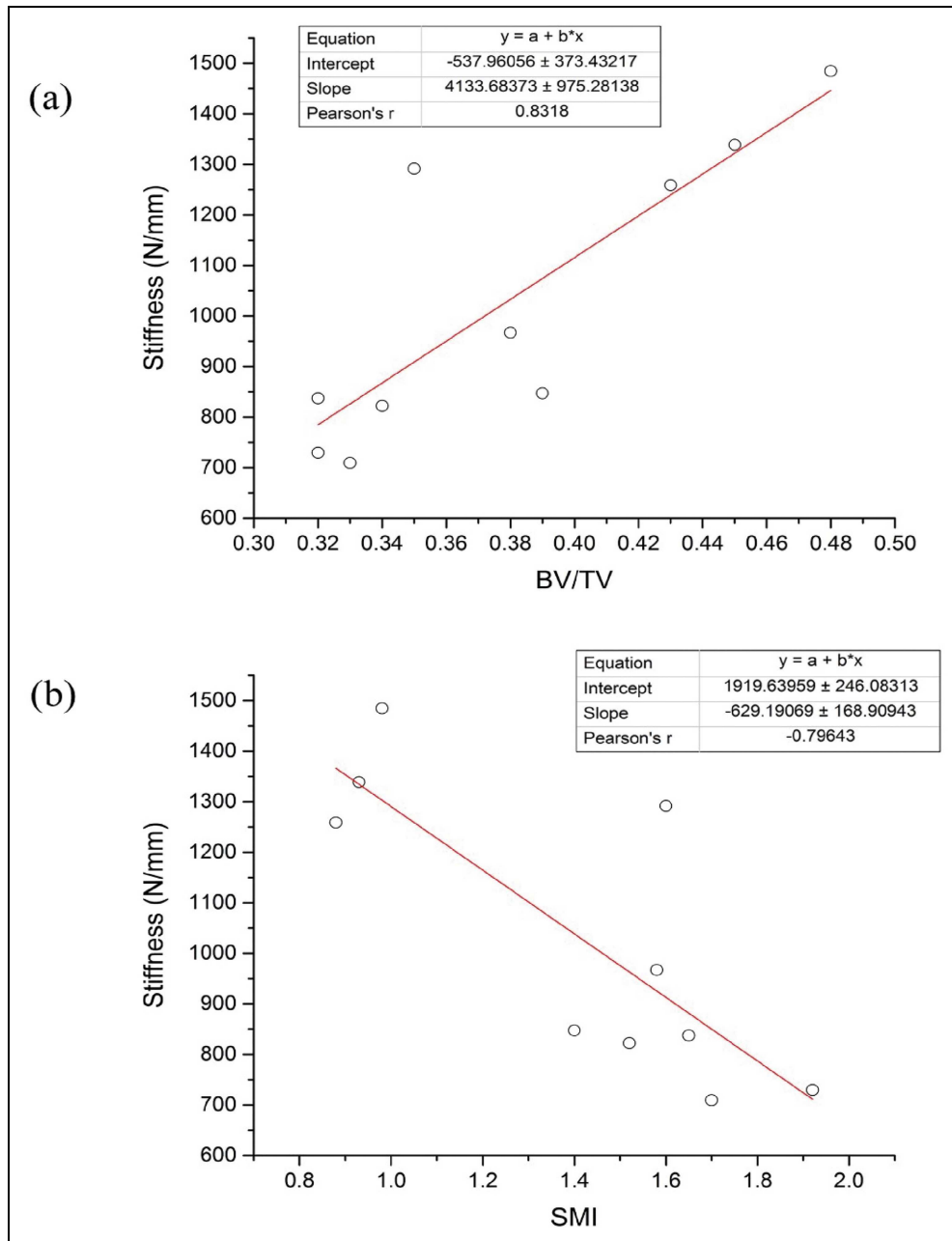


Figure 13. Linear relationship between (a) BV/TV and (b) SMI with stiffness.

have an apparent transition of microarchitecture, which is from plate like to rod-like structure.⁴⁷ Stein et al.⁴⁹ in their study found that the bone stiffness related with trabecular connectivity, trabeculae orientation and trabecular plates. Thus, in correspondence to previous studies, our results suggest that plate-like trabecular structure (lower SMI value) can contribute to higher trabecular stiffness.

There are a few limitations in the interpretation of results that should be considered. This study has employed trabecular samples from anatomic site of bovine femoral bone. As such, the microarchitecture parameters may differ from that of the human bone or other anatomic sites. However, there are a few works done that demonstrate agreement between the architecture as well as mechanical properties of bovine trabecular bone

and that of a healthy human.^{50,51} Furthermore, the impact of marrow phase on the trabecular structure can be further investigated in terms of its properties such as the variation of constituents and viscosity.

In summary, this study was investigated on the correlation of the morphology parameters onto the mechanical properties of trabecular bone with presence of bone marrow. The bone volume fraction and SMI were identified as the one that has a higher correlation with the trabecular permeability and stiffness compared with others morphological parameters. Moreover, the bone marrow behaviour through the physiological activity was identified in this study. This study provides insight into understanding how human daily physiological activities contribute to the bone remodelling process and nutrient transport with

the bone environment. However, more knowledge in this area was crucial to studying the bone adaption to the bone replacement and in estimating fracture risk.

Conclusion

The overall aim of this study was to assess the importance on the interaction between the bone marrow and trabecular bone structure during mechanical loading by using the FSI approach. Trabecular bone is known as a highly porous structure with a significant volume of bone marrow, a compressive or tensile force on the trabecular bone will result in bone marrow movement with respect to the trabecular bone structure. It is believed that the fluid flow will cause the shear stress to the trabecular structure. The interaction between the fluid and trabecular bone will occur, and this incident might have several effects on the trabecular structure. Moreover, bone remodelling process was occurring due to the shear stress on the bone cell which triggers the process. In addition to shear stress, based on previous study the hydraulic stiffening effect occurs due to the presence of bone marrow within the trabecular bone structure. Therefore, this study proposed the used of FSI approach to model the trabecular bone behaviour and marrow flow characteristic.

The physiological activities in daily human life play a major role than calcium intake in the bone development process.⁵² It contributes to mechanical stimuli in bone marrow and trabecular bone strain. Normal walking is one of human major daily activity is chosen in this study as a boundary condition in analysing the trabecular bone behaviour. The bone marrow behaviour was recorded during the normal walking cyclic loading. While the trabecular bone deforms according to the physiological load, the bone marrow within will encounter mechanical stimulation in mechanobiological response.^{53,54} The shear stress value along normal walking gait loading was found in a range of 0.05 to 0.27 Pa which is sufficient to regulate cell response minimally.³³ However, due to ageing factor, bone resorption rate will become higher. Thus, higher shear stress was needed in order to have rapid bone remodelling process to encounter the bone resorption rate. Furthermore, this study also provides insight into understanding the related mechanobiological of bone cells and disease in deterioration of nutrient supplied to the bone.

Acknowledgements

This project was sponsored by the Universiti Teknologi Malaysia (UTM) and Universitas Airlangga (Unair) through the Grant scheme (R.J130000.7309.4B535) matching grant scheme. The authors would also like to thank the Research Management Centre, Universiti Teknologi Malaysia, for managing the project.

Declaration of conflicting interests

GQ3 The author(s) declared no potential conflicts of interest with respect to the research, authorship, and/or publication of this article.



GQ3 = OK

Funding

The author(s) disclosed receipt of the following financial support for the research, authorship, and/or publication of this article: This work was supported by the Universiti Teknologi Malaysia, (grant number R.J130000.7309.4B535).

AQ1 = correct

ORCID iDs

Andreas Öchsner  <https://orcid.org/0000-0002-8844-3206> **GQ6**
Ardiyansyah Syahrom  <https://orcid.org/0000-0001-7278-5861>

GQ6 = ok

References

1. Saad APM and Syahrom A. Study of dynamic degradation behaviour of porous magnesium under physiological environment of human cancellous bone. *Corros Sci* 2018; 131: 45–56.
2. Yourek G, McCormick SM, Mao JJ, et al. Shear stress induces osteogenic differentiation of human mesenchymal stem cells. *Regen Med* 2010; 5: 713–724.
3. Coughlin TR and Niebur GL. Fluid shear stress in trabecular bone marrow due to low-magnitude high-frequency vibration. *J Biomech* 2012; 45: 2222–2229.
4. Vaughan T, Voisin M, Niebur G, et al. Multiscale modeling of trabecular bone marrow: understanding the micromechanical environment of mesenchymal stem cells during osteoporosis. *J Biomech Eng* 2015; 137. **page: 1-10** **AQ2**
5. You L, Cowin SC, Schaffler MB, et al. A model for strain amplification in the actin cytoskeleton of osteocytes due to fluid drag on pericellular matrix. *J Biomech* 2001; 34: 1375–1386.
6. Adachi T, Kameo Y and Hojo M. Trabecular bone remodeling simulation considering osteocytic response to fluid-induced shear stress. *Philosophical transactions of the royal society A: mathematical. Phys Eng Sci* 2010; 368: 2669–2682.
7. Wittkowske C, Reilly GC, Lacroix D, et al. In vitro bone cell models: impact of fluid shear stress on bone formation. *Front Bioeng Biotechnol* 2016; 4: 87.
8. Birmingham E, Niebur G, McNamara L, et al. An experimental and computational investigation of bone formation in mechanically loaded trabecular bone explants. *Ann Biomed Eng* 2016; 44: 1191–1203.
9. Shen V, Liang X, Bircham R, et al. Short term immobilization-induced cancellous bone loss is limited to regions undergoing high turnover and/or modeling in mature rats. *Bone* 1997; 21: 71–78.
10. Rodriguez N, Herndon D and Klein G. Evidence against a role of immobilization in the bone loss following burns. *Bone* 2011; 2: S190.
11. Frost HM. Wolff's Law and bone's structural adaptations to mechanical usage: an overview for clinicians. *Angle Orthod* 1994; 64: 175–188.
12. Frost HM. Bone "mass" and the "mechanostat": a proposal. *Anat Rec* 1987; 219: 1–9.
13. Burr DB, Milgrom C, Fyhrie D, et al. In vivo measurement of human tibial strains during vigorous activity. *Bone* 1996; 18: 405–410.
14. Fritton SP, McLeod KJ and Rubin CT. Quantifying the strain history of bone: spatial uniformity and self-similarity of low-magnitude strains. *J Biomech* 2000; 33: 317–325.
15. Gurkan UA and Akkus O. The mechanical environment of bone marrow: a review. *Ann Biomed Eng* 2008; 36: 1978–1991.

16. McAllister T and Frangos J. Steady and transient fluid shear stress stimulate NO release in osteoblasts through distinct biochemical pathways. *J Bone Miner Res* 1999; 14: 930–936.
17. Li YJ, Batra NN, You L, et al. Oscillatory fluid flow affects human marrow stromal cell proliferation and differentiation. *J Orthop Res* 2004; 22: 1283–1289.
18. Knight MN and Hankenson KD. Mesenchymal stem cells in bone regeneration. *Adv Wound Care* 2013; 2: 306–316.
19. Shao J, Zhang W and Yang T. Using mesenchymal stem cells as a therapy for bone regeneration and repairing. *Biol Res* 2015; 48: 62.
20. Castillo AB and Jacobs CR. Mesenchymal stem cell mechanobiology. *Curr Osteoporos Rep* 2010; 8: 98–104.
21. Klein-Nulend J, Van Der Plas A, Semeins CM, et al. Sensitivity of osteocytes to biomechanical stress in vitro. *FASEB J* 1995; 9: 441–445.
22. Case N, Sen B, Thomas J, et al. Steady and oscillatory fluid flows produce a similar osteogenic phenotype. *Calcif Tissue Int* 2011; 88: 189–197.
23. Bakker AD, Joldersma M, Klein-Nulend J, et al. Interactive effects of PTH and mechanical stress on nitric oxide and PGE2 production by primary mouse osteoblastic cells. *Am J Phys-Endocrinol Metab* 2003; 285: E608–EE13.
24. Arnsdorf EJ, Tummala P, Kwon RY, et al. Mechanically induced osteogenic differentiation—the role of RhoA, ROCKII and cytoskeletal dynamics. *J Cell Sci* 2009; 122: 546–553.
25. Yeatts AB and Fisher JP. Bone tissue engineering bioreactors: dynamic culture and the influence of shear stress. *Bone* 2011; 48: 171–181.
26. Bergmann G, Deuretzbacher G, Heller M, et al. Hip contact forces and gait patterns from routine activities. *J Biomech* 2001; 34: 859–871.
27. Fatihhi S, Harun M, Kadir MRA, et al. Uniaxial and multi-axial fatigue life prediction of the trabecular bone based on physiological loading: a comparative study. *Ann Biomed Eng* 2015; 43: 2487–2502.
28. Homminga J, McCreddie BR, Weinans H, et al. The dependence of the elastic properties of osteoporotic cancellous bone on volume fraction and fabric. *J Biomech* 2003; 36: 1461–1467.
29. Sylvester AD and Kramer PA. Young's modulus and load complexity: modeling their effects on proximal femur strain. *Anat Rec* 2018; 301: 1189–1202.
30. Bayraktar HH, Gupta A, Kwon RY, et al. The modified super-ellipsoid yield criterion for human trabecular bone. *J Biomech Eng* 2004; 126: 677–684.
31. Bryant J, David T, Gaskell P, et al. Rheology of bovine bone marrow. Proceedings of the institution of mechanical engineers. Part H: *J Eng Med* 1989; 203: 71–75.
32. Haskill JS, McNeill TA and Moore MAS. Density distribution analysis of In vivo and In vitro colony forming cells in bone marrow. *J Cell Physiol* 1970; 75: 167–179.
33. Kreke MR, Sharp LA, Woo Lee Y, et al. Effect of intermittent shear stress on mechanotransductive signaling and osteoblastic differentiation of bone marrow stromal cells. *Tissue Eng, Part A* 2008; 14: 529–537.
34. Nauman E, Satcher R, Keaveny T, et al. Osteoblasts respond to pulsatile fluid flow with short-term increases in PGE2 but no change in mineralization. *J Appl Physiol* 2001; 90: 1849–1854.
35. McKercher CM, Schmidt MD, Sanderson KA, et al. Physical activity and depression in young adults. *Am J Prev Med* 2009; 36: 161–164.
36. Krumm EM, Dessieux OL, Andrews P, et al. The relationship between daily steps and body composition in postmenopausal women. *J Womens Health (Larchmt)* 2006; 15: 202–210.
37. Welch R, Johnston 2nd C, Waldron M, et al. Bone changes associated with intraosseous hypertension in the caprine tibia. *JBJS* 1993; 75: 53–60.
38. Hu M, Cheng J and Qin Y-X. Dynamic hydraulic flow stimulation on mitigation of trabecular bone loss in a rat functional disuse model. *Bone* 2012; 51: 819–825.
39. Teo J, Si-Hoe K, Keh J, et al. Correlation of cancellous bone microarchitectural parameters from microCT to CT number and bone mechanical properties. *Mater Sci Eng C* 2007; 27: 333–339.
40. Baroud G, Falk R, Crookshank M, et al. Experimental and theoretical investigation of directional permeability of human vertebral cancellous bone for cement infiltration. *J Biomech* 2004; 37: 189–196.
41. Liebschner MA and Keller TS. Hydraulic strengthening affects the stiffness and strength of cortical bone. *Ann Biomed Eng* 2005; 33: 26–38.
42. Kohles SS and Roberts JB. Linear poroelastic cancellous bone anisotropy: trabecular solid elastic and fluid transport properties. *J Biomech Eng* 2002; 124: 521–526.
43. ~~Lopez KW, Goldstein SA, Ciarelli MJ, et al. The relationship between the structural and orthogonal compressive properties of trabecular bone. 1994.~~ AQ3
44. Goldstein AS, Juarez TM, Helmke CD, et al. Effect of convection on osteoblastic cell growth and function in biodegradable polymer foam scaffolds. *Biomaterials* 2001; 22: 1279–1288.
45. Syahrom A, Kadir MRA, Abdullah J, et al. Permeability studies of artificial and natural cancellous bone structures. *Med Eng Phys* 2013; 35: 792–799.
46. Hildebrand T and Rüeggsegger P. Quantification of bone microarchitecture with the structure model index. *Comput Methods Biomech Bio Med Eng* 1997; 1: 15–23.
47. Wang J, Zhou B, Liu XS, et al. Trabecular plates and rods determine elastic modulus and yield strength of human trabecular bone. *Bone* 2015; 72: 71–80.
48. Wang J, Zhou B, Parkinson I, et al. Trabecular plate loss and deteriorating elastic modulus of femoral trabecular bone in intertrochanteric hip fractures. *Bone Res* 2013; 1: 346–354.
49. Stein EM, Kepley A, Walker M, et al. Skeletal structure in postmenopausal women with osteopenia and fractures is characterized by abnormal trabecular plates and cortical thinning. *J Bone Miner Res* 2014; 29: 1101–1109.
50. Keaveny TM, Wachtel EF, Ford CM, et al. Differences between the tensile and compressive strengths of bovine tibial trabecular bone depend on modulus. *J Biomech* 1994; 27: 1137–1146.
51. Morgan EF, Yeh OC, Chang WC, et al. Nonlinear behavior of trabecular bone at small strains. *J Biomech Eng* 2001; 123: 1–9.
52. Anderson JJ. The important role of physical activity in skeletal development: how exercise may counter low calcium intake. *Am J Clin Nutr* 2000; 71: 1384–1386.
53. Metzger TA, Schwaner SA, LaNeve AJ, et al. Pressure and shear stress in trabecular bone marrow during whole bone loading. *J Biomech* 2015; 48: 3035–3043.
54. Birmingham E, Grogan J, Niebur G, et al. Computational modelling of the mechanics of trabecular bone and marrow using fluid structure interaction techniques. *Ann Biomed Eng* 2013; 41: 814–826.

Influence of Bone Marrow Characteristic and Trabecular Bone Morphology on Bone Remodelling Process with FSI Approach

Journal:	<i>Part L: Journal of Materials: Design and Applications</i>
Manuscript ID	JMDA-21-0617.R2
Manuscript Type:	Original article
Date Submitted by the Author:	n/a
Complete List of Authors:	<p>Abdul Rahim, Rabiatul; Universiti Teknologi Malaysia - Main Campus Skudai, Medical Devices and Technology Centre (MEDiTEC) Rianti, Devi ; Universitas Airlangga Fakultas Kedokteran Gigi, Dental materials science MOHD SZALI JANUDDI, MOHD AL ; Universiti Kuala Lumpur, FACILITIES MAINTENANCE ENGINEERING (FaME) SECTION Md Saad, Amir Putra; Universiti Teknologi Malaysia, Schhol of Mechanical Engineering; Medical Devices and Technology Centre (MEDITEC); Institute of Human Centred and Engineering (iHumEn) Zakaria, Zulfadzli ; Universiti Teknologi Malaysia, Medical Devices and Technology Centre (MEDiTEC) Yuliati, Anita ; Universitas Airlangga, dental materials science Abdul Kadir, Mohammed ; Universiti Teknologi Malaysia - Main Campus Skudai, Medical Devices and Technology Centre (MEDITEC) Öchsner, Andreas; Esslingen University of Applied Sciences, Faculty of Mechanical and Systems Engineering ZAMAN, TUNKU; Universiti Malaya, Department of Orthopaedic Surgery, Faculty of Medicine Saqr, Khalid; Arab Academy for Science Technology and Maritime Transport College of Computing and Information Technology, Mechanical of Engineering Syahrom, Ardiyansyah; Universiti Teknologi Malaysia - Main Campus Skudai, Medical Devices and Technology Centre (MEDiTEC); Universiti Teknologi Malaysia, Applied Mechanics and Design</p>
Keywords:	Fluid Structure Interaction, Trabecular Bone, Bone Marrow, Shear Stress, Stiffness, Bone Remodelling
Abstract:	<p>While doing daily physiological activities, the trabecular bone will experience a certain amount of deformation which leads to the bone marrow movement. The movement can affect the bone remodelling process and the properties of the bone itself. The bone marrow plays a role as a hydraulic stiffening of the trabecular structure. However, previous studies analysed on trabecular bone and bone marrow separately, which is not considered as the actual condition. Thus, it is crucial to consider combine analyses of the bone marrow with the trabecular structure simultaneous. The aim of this study is to investigate the effect of bone marrow on the mechanical environment and the structure of trabecular bone during normal walking loading. Hence, this study used the Fluid-Structure Interaction (FSI) approach as a finite element method to discover the effect of bone marrow to the trabecular structure and vice versa. The findings show the shear stress value along normal walking phase was found in a range of 0.01-0.27 Pa which is sufficient to regulated cell response minimally. This study provides</p>

1
2
3
4
5
6
7
8
9
10
11
12
13
14
15
16
17
18
19
20
21
22
23
24
25
26
27
28
29
30
31
32
33
34
35
36
37
38
39
40
41
42
43
44
45
46
47
48
49
50
51
52
53
54
55
56
57
58
59
60

	insight into understanding the related mechanobiological responds towards supply of nutrients onto bone cells.

SCHOLARONE™
Manuscripts

1
2
3 **1 Influence of Bone Marrow Characteristic and Trabecular Bone Morphology on Bone**
4 **2 Remodelling Process with FSI Approach**
5
6
7 3

8 4 A.A.R Rabiatul¹, Devi Rianti^{3*}, S.J. Fatihhi⁴, Amir Putra Md Saad², Zulfadzli Zakaria¹, Anita
9 Yuliati³, M.N. Harun^{2,5}, M.R.A. Kadir^{5,6}, Andreas Öchsner⁷, Tunku Kamarul⁸, Khalid M.
10 Saqr⁹, Ardiyansyah Syahrom^{1,2*}
11
12 6
13 7

14 8 *¹Medical Device Technology Center (MEDiTEC), Institute Human Centred Engineering*
15 *(iHumEn), Universiti Teknologi Malaysia, Johor, Malaysia*
16 9

17 10 *²School of Mechanical Engineering, Faculty of Engineering, Universiti Teknologi Malaysia,*
18 *Johor, Malaysia*
19 11

20 12 *³Dental materials science Department, Faculty of Dentistry Medicine, Universitas Airlangga*
21 *Surabaya, Jawa Timur, Indonesia*
22 13

23 14 *⁴Universiti Kuala Lumpur, Malaysian Institute of Industrial Technology*

24 15 *⁵Sports Innovation and Technology Centre (SITC), Institute Human Centred Engineering*
25 *(iHumEn), Universiti Teknologi Malaysia, Johor, Malaysia*
26 16

27 17 *⁶School of Biomedicals Engineering and Health Sciences, Faculty of Engineering, Universiti*
28 *Teknologi Malaysia, Johor, Malaysia*
29 18

30 19 *⁷Lightweight Design / Structural Simulation, Faculty of Mechanical Engineering, Esslingen*
31 *University of Applied Sciences, Esslingen, Germany*
32 20

33 21 *⁸Tissue Engineering Group (TEG), National Orthopaedic Centre of Excellence in Research*
34 *and Learning (NOCERAL), Department of Orthopaedic Surgery, Faculty of Medicine,*
35 *University of Malaya, Kuala Lumpur, Malaysia*
36 22

37 23 *⁹College of Engineering and Technology, Arab Academy for Science, Technology and*
38 *Maritime Transport, Alexandria, Egypt*
39 24

40 25
41 26
42 27 *Corresponding author:

43 28 Ardiyansyah Syahrom
44 29 Medical Device Technology Center (MEDiTEC),
45 30 Institute Human Centred Engineering (iHumEn),
46 31 Universiti Teknologi Malaysia
47 32 Email: ardiyans@gmail.com

48 33 Devi Rianti
49 34 Dental materials science Department,
50 35 Faculty of Dentistry Medicine,
51 36 Universitas Airlangga
52 37 Surabaya, Jawa Timur, Indonesia
53
54
55
56
57
58
59
60

38 **Abstract**

39 While doing daily physiological activities, the trabecular bone will experience a certain amount of
40 deformation which leads to the bone marrow movement. The movement can affect the bone remodelling
41 process and the properties of the bone itself. The bone marrow plays a role as a hydraulic stiffening of
42 the trabecular structure. However, previous studies analysed on trabecular bone and bone marrow
43 separately, which is not considered as the actual condition. Thus, it is crucial to consider combine
44 analyses of the bone marrow with the trabecular structure simultaneous. The aim of this study is to
45 investigate the effect of bone marrow on the mechanical environment and the structure of trabecular
46 bone during normal walking loading. Hence, this study used the Fluid-Structure Interaction (FSI)
47 approach as a finite element method to discover the effect of bone marrow to the trabecular structure
48 and vice versa. The findings show the shear stress value along normal walking phase was found in a
49 range of 0.01-0.27 Pa which is sufficient to regulated cell response minimally. This study provides
50 insight into understanding the related mechanobiological responds towards supply of nutrients onto
51 bone cells.

52 Keyword: Fluid Structure Interaction, Trabecular Bone, Bone Marrow, Shear Stress, Stiffness, Bone
53 Remodelling

55 **1.0 INTRODUCTION**

57 Physiological loading induced trabecular bone deformation that leads to the bone marrow
58 movement within the porous structure which contribute to stimulating the osteogenic response to the
59 bone cells (1). The forces from the physiological loading cause both small strain and shear stress which
60 known as a key to initiate the bone remodelling process (2-5). Currently, researchers tried to discover
61 the actual value necessary to stimulate the bone cells for the bone remodelling process. To this date,
62 experimental and simulation study have been performing in order to capture the value of these
63 biomechanical stimuli that encourage the remodelling process (6-8). Bone marrow is a prime
64 component in trabecular bone, in which it accommodates bone predecessors' cells for bone remodelling.
65 Thus, it is important to consider its presence to better represent the actual conditions of trabecular bone.
66 Therefore, knowledge of biomechanical environment that occur within the trabecular bone during daily
67 physiological activities is necessary to comprehend on how the bone marrow can affect the bone
68 remodelling.

69 Physiological loading includes daily activities such as house chores, daily walking, and sports
70 activity helps in maintaining the bone health by transferring force to the bone structure. These can be
71 seen on immobilization and bedrest individual that had reduce in their bone mass (9, 10). These
72 relationship of loading and bone formation had been support with the Wolff's law since 1892 (11). The

1
2
3 73 trabecular bone experience compression and tension in the microstructure due to the loading causing
4 74 the micro strain which one of the mechanical stimuli. Previous study reported that the physiological
5 75 activities initiate in range of 0.001-0.003 mm/mm on the trabecular structure (12, 13). However,
6 76 minimal physiological activity cause $1000\mu\epsilon$ which cause bone resorption process higher compare to
7 77 the bone resorption (14). Amazingly the bone can heal itself when there is external loads act upon the
8 78 cells which can help in cells excite by signalling to the bones to start building themselves up. Then
9 79 again, the loads from human daily life will also initiate the movement of bone marrow within the
10 80 structure which cause the shear stress that act as response to the remodelling process (15).

11
12
13
14
15
16 81 The osteogenic response include osteoprogenitor cells secrete autocrine factors, for example
17 82 prostaglandins E_2 (PGE_2) and nitric oxide (NO), which can regulate the remodelling activity (16). In
18 83 addition, the proliferation rates have been found increasing when the bone marrow stromal cells were
19 84 exposed to the fluid flow, which means higher number of cells participate in bone formation (17). The
20 85 mesenchymal stem cells (MSCs) has been actively investigate in experiment and simulation due to its
21 86 ability to differentiate into other cells such as osteoblast (bone cells), chondrocytes (cartilage cells) and
22 87 adipocytes (fat cells) (18-20). The shear stress known as one of the parameters required for the MSCs
23 88 in the bone marrow to differentiate and assists the remodelling activity (20, 21). The range of shear
24 89 stress need for the cells to response mention by previous study is about 0.02 to 1.0 Pa (2, 22-25).
25 90 Undoubtedly, bone remodelling process also requires adequate nutrient transport through the bone cells.
26 91 These were also with help of bone marrow which function to transport the nutrient and remove waste.
27 92 However, knowledge on how shear stress value contributing in MSCs to differentiate to different cells
28 93 are still shallow.

29
30
31
32
33
34
35
36
37 94 In the present work the movement of the bone marrow regulate osteogenic responds which
38 95 relate to the trabecular bone deformation due to the physiological activity. Thus far, the is no study
39 96 using physiological gait loading as boundary to examine the effect of interaction on mechanical stimulus
40 97 and trabecular bone. Therefore, the aim of this study is to investigate the effect of bone marrow
41 98 mechanical environment and trabecular bone structure during normal walking loading. A fluid structure
42 99 interaction (FSI) approach was applied to determine the deformation of trabecular bone with
43 100 corresponding of marrow shear stress in bone remodelling activity.

44 45 46 47 48 49 101 **2.0 MATERIALS AND METHODS**

50 51 102 **2.1 SAMPLE PREPARATION**

52
53 103 The fresh bovine femur bones were harvested from the local slaughterhouse and kept frozen at -18°C
54 104 to 26°C . Specimens of trabecular bone were taken by using a Bosch circular saw with copious water
55 105 irrigation. The femur bone was then divided and cut into a section of medial condyle, femoral neck and
56 106 femoral ball with the vertical orientation due to the maximum extension of knee joint occurred. The
57 107 trabecular bone was then again cut into a cubic shape (10mm x 10mm x 17mm) in length by using a

1
2
3 108 precision cutting tool (Allied Techcut, USA). The precision cutter consists of diamond-resin bonded
4
5 109 wafering blade with a minimum speed of 150-250 rpm with continuously water irrigation to prevent
6
7 110 heat-related damages. Then, the specimens were placed in small airtight plastic bag with the purpose of
8
9 111 reducing the thermal cycling and stored in the freezer with a temperature below -26°C. After that, the
10
11 112 specimens will go through next procedure using the ultrasonic cleaner (Crest ultrasonic, model
12
13 113 P11000SR, USA) additional with a chemical detergent (Pumicizedcitrius, Gent-l-kleen,USA) to
14
15 114 cleaned from marrow. The specimens were then submerged for about 10-15 minutes at a temperature
16
17 115 below 46°C. In order to remove the loose particles and excessive marrow, the specimens were then air-
18
19 116 jetted and vacuumed suction. This procedure was repeated until all excessive marrow is removed
20
21 117 (Fatihhi SJ et al., 2015). A custom jig was used to align the specimen for improved vertical oriented.
22
23 118 Afterwards, the specimens sealed in an airtight bag placed in a -20°C freezer and frozen overnight while
24
25 119 the adhesive completely cured. Only then, the samples are scan by using the μ -CT scanner (SkyScan
26
27 120 1172, Bruker MicroCT, Belgium).

2.2 MODEL DEVELOPMENT

27 122 The two-dimensional image data sets from the μ -CT scan were stacked in sequence by Mimics software
28
29 123 (MIMICS 12, Materialise, Belgium) and converted into rectangular shape to construct the trabecular
30
31 124 model. The thickness of each images slice is 15 μ m. The stacked image datasets were calculated into
32
33 125 three-dimensional trabecular model through image segmentation by the Mimics software.
34
35 126 Subsequently, the image datasets were thresholded to select the region of interest for three-dimensional
36
37 127 constructed model. In addition, by using an adapted marching cubes algorithm, the triangular surface
38
39 128 meshes were generated for the trabecular model. Then again, the result of triangular surface mesh was
40
41 129 very fine, which needed to follow with step of removing noise, redundant parts and irregularities shape
42
43 130 to construct accurate three-dimensional models. There were 10 models generated and tested in this
44
45 131 study.

44 132 As for finite element analysis simulation, small sized sub volume region of interest was selected from
45
46 133 the fine mesh trabecular bone constructed models (Figure 1) due to the limitation of computer capability
47
48 134 to complete the simulation study. These models were then converted into finite element mesh for the
49
50 135 simulation. In addition, the trabecular bone model surface meshes with jagged or bad sector are also
51
52 136 repaired before importing the model. For the FSI study purpose, the outer wall of the models needed to
53
54 137 convert into a flat surface. Thus, for the model preparation, the smaller size sub-models were then
55
56 138 merged with cube surface mesh in the Mimics software. After that, the uneven surface of trabecular sub
57
58 139 volume models was removed according to the sub volume model shape. Then, the space between the
59
60 140 sub model and the cube were stitch together by creating a triangular mesh in between the space. These
141
142 steps were applied to all six surfaces for the sub trabecular model. Finally, the surface mesh is exported
to an STL format file.

1
2
3 143 **Figure 1:** Development of three-dimensional model into sub volume model.
4
5 144

6 145 **2.3 MORPHOLOGY STUDY**

8 146

9 147 From the μ -CT scan images, the morphological study was conducted. One of a trabecular bone sample
11 148 contains approximately 900 image slices (Figure 2 (b)). The morphological indices were measured
12 149 using ImageJ (ImageJ, National Institute of Health, USA). All these slices were import and stacked
14 150 (Figure 2 (a)) by using BoneJ plugins in ImageJ software to obtain the trabecular morphological data.
16 151 The parameters measured included BV/TV, Tb.Th, Tb.Sp, Tb.N, DA, MIL, etc. All data present in
17 152 Table 1.
19 153

20 154 **Figure 2:** Images obtain from μ -CT scan with (a) Images stacked in sequence according to sample
22 155 orientation (b) raw scanned images file
24 156

26 157 **Table 1:** Morphological indices of trabecular bone sample
27 158

29 159 **2.4 COMPUTATIONAL SIMULATION**

31 160

32 161 Two-way fluid-structure analysis were conducted using COMSOL Multiphysics software with purpose
34 162 of investigate the fluid behaviour of bone marrow under gait loading conditions. A gait loading which
35 163 representing normal walking were applied through the cap faces feature which considered as a rigid
37 164 body. The gait loading (Figure 3) applied in multi-axis according to normal walking phase (26). The
39 165 normal walking phase of gait cycle was divided into 40 discrete points for the simulation. The cap faces
40 166 feature is vital in the FSI study due to restriction coupling between the trabecular model and marrow
42 167 model within the FEA. In addition, the prescribed displacement was applied to the cap, where the
43 168 domain was restricted in the X and Y directions (Figure 4). As for the fluid boundary, the plane of the
45 169 bottom boundary of fluid was applied as symmetry in order to ensure that the marrow volume remains
46 170 within the domain when there is load applied through the structure. Moreover, in order to prevent
48 171 normal velocity to the respective boundary, the marrow flow was model as symmetric in their normal
49 172 directions. The convergence analysis in this study conclude that 400 thousand tetrahedral elements and
51 173 shape function was used tessellation method is Delaunay on average were needed for accurate result
52 174 computation (see Figure 5). In addition, the FSI interface uses an arbitrary Lagrangian-Eulerian (ALE)
54 175 method, which allows moving boundaries without the need for the mesh movement to follow the
56 176 material. This ALE method combined the fluid flow formulated using a Eulerian description and a
57 177 spatial frame with solid mechanics formulated using a Lagrangian description and a material frame.
59 178 The analysis was performed with the criterion of the von Mises stress criterion less than 5%.

1
2
3 **Figure 3:** Gait loading of normal walking based on body weight percentage (Bergmann G. et al.,
4
5 180 2001).

6 181

7
8 182 The time-dependent solution is obtained for every gait cycle. Details on the force parameters
9
10 183 implemented in this study was demonstrated in (27). The solid trabecular structures were modelled as
11 184 a linear elastic material (28). An elastic modulus (E) of 1000 MPa (29) and Poisson's ratio of 0.3 was
12
13 185 attributed to the trabecular bone solid structure (30). Additionally, the viscosity of fluid marrow was
14 186 assigned 0.4 Pa.s and modelled as incompressible according to Bryant et al. (31), Newtonian fluid with
15
16 187 density of 1060 kg/m³ (32). The surface between the trabecular structure and marrow fluid is assigned
17
18 188 as no-slip boundary.

19 189

20
21 190 **Figure 4** Boundary Conditions (BC) of trabecular bone and bone marrow models

22 191

23
24 192 **Figure 5** Convergence study for the trabecular structure model

25 193

26
27 194 In the present work, the bone marrow was modelled as an incompressible liquid. The incompressible
28
29 195 Navier-Stokes equation was considered as the governing equation, in which;

$$\nabla \cdot \mathbf{u}_{fluid} = 0 \quad (1)$$

30
31 196

32
33 197 On the other hand, the momentum equation was as follows;

$$\rho \frac{\partial \mathbf{u}_{fluid}}{\partial t} + \rho (\mathbf{u}_{fluid} \cdot \nabla) \mathbf{u}_{fluid} = \nabla \cdot [-p\mathbf{I} + \mu(\nabla \mathbf{u}_{fluid} + (\nabla \mathbf{u}_{fluid})^T)] + \mathbf{F} \quad (2)$$

34
35 198

36
37
38 199 where the external force acting on the fluid was denoted by \mathbf{F} , and gravity was neglected. Meanwhile,
39
40 200 equation for solid at local equilibrium is given by;

$$\rho \frac{\partial^2 \mathbf{u}_{solid}}{\partial t^2} - \nabla \cdot \boldsymbol{\sigma} = \mathbf{F}_v \quad (3)$$

41
42 201

43
44
45 202 where $\boldsymbol{\sigma}$ and \mathbf{F}_v are the Cauchy stress tensor and body force, respectively. Deformed structure was
46
47 203 demonstrated by \mathbf{u}_{solid} , whereas the Piola-Kirchhoff stress, \mathbf{S} was used to calculate the Cauchy stress
48
49 204 using the following equation;

$$\boldsymbol{\sigma} = J^{-1} \mathbf{F} \mathbf{S} \mathbf{F}^T. \quad (4)$$

50
51 205

52
53 206 Using the gradient of displacement vector \mathbf{u}_{solid} , the deformation gradient, \mathbf{F} can be expressed as;

$$\mathbf{F} = (\mathbf{I} + \nabla \mathbf{u}_{solid}), \quad (5)$$

54
55 207

56
57
58
59
60

208 In which the identity matrix was denoted by \mathbf{I} , and the Jacobian of the deformation is defined as;

$$J = \det(\mathbf{F}). \quad (6)$$

210 Fluid domain was solved based on Eulerian formulation, while solid domain was solved based on
211 Lagrangian formulations. In coupling fluid-solid system, the arbitrary Lagrangian-Eulerian method
212 can be implemented with total force on the fluid-solid boundary was given as;

$$f_r = \mathbf{n} \cdot \left[-p\mathbf{I} + \mu(\nabla\mathbf{u}_{fluid} + (\nabla\mathbf{u}_{fluid})^T) \right], \quad (7)$$

214 With \mathbf{n} is the normal acting outward at the boundary, the force at the structure's boundary is given by;

$$\mathbf{F}_r = \boldsymbol{\sigma} \cdot \mathbf{n}. \quad (8)$$

216 In Spatial and material coordinate system, these forces can be coupled thru a force transformation using
217 the arbitrary Eulerian-Lagrangian method as follows:

$$\mathbf{F}_r = f_r \cdot \frac{dv}{dV}. \quad (10)$$

219 Mesh element scale factors dv and dV are the fluid and material frames, respectively. Further, the
220 relationship of structural velocity of the moving wall with the fluid velocity is demonstrated as follows:

$$\mathbf{u}_{fluid} = \mathbf{u}_w, \quad (11)$$

222 Thus, the rate of change of the solid displacement is defined by the structural velocity.

$$\mathbf{u}_w = \frac{\partial \mathbf{u}_{solid}}{\partial t} \quad (12)$$

224 2.5 STATISTICAL ANALYSIS

225 All morphology indices are presented in mean and standard deviation (Table 1). The Pearson's
226 correlation and linear regression analysis were performed to explore the interrelationship between
227 the morphological indices and the mechanical properties of the trabecular bone sample. The
228 multiple linear regression was perform using IBM SPSS Statistics 23 (IBM Corp, USA). For all
229 comparison, the level of significant for p-value was <0.05.

230 3.0 RESULTS

232 The average von Mises stress distribution during normal walking with cycle duration was plotted
233 as shown in Figure 6. The peak pressure reached as high as 11.35×10^5 Pa. Then again, the minimum
234 stress for trabecular bone is 10.75×10^4 Pa at period of 0.86s. As can be seen, the behaviour of von
235 Mises stress during gait cycle is similar to the force in the vertical direction. From the computational

1
2
3 236 FSI simulation, the von Mises stress distribution within the trabecular bone model along gait normal
4 walking gait loading cycle at different time frame as illustrated in Figure 7. Comparing Figure 7(a) and
5 237 (b), more area covered with high stresses at time 0.14 s. These results match with the graph of the von
6 238 Mises stress over time.
7
8 239

9 240

10
11 241 **Figure 6:** von Mises stress distribution on the trabecular bone during normal walking

12 242

13
14 243 **Figure 7:** Comparison of von Mises stress on the trabecular bone at different time frame (a) $t = 0.14$ s
15 244 and (b) $t = 0.86$ s
16

17 245

18
19 246 The pressure and shear stress distribution during gait loading cycle are presented in Figure 8. This
20 247 figure shows how the structure of trabecular bone affects the fluid characteristic during the gait loading
21 248 cycle. It can be observed from the Figure 8 that the pattern of pressure distribution was similar to the
22 249 von Mises stress results. The pressure was range from 380 to 4070 Pa during the normal walking cycle.
23
24 250 Moreover, as discussed earlier, the trabecular structure experience shear stress due to bone marrow
25 251 movement. With an average of 0.09 Pa, the shear stress was in the range of 0.01 to 0.27 Pa.
26
27 252

28 253

29
30 254 Based on 2D images of the trabecular model cross section, the pressure on top section was lower than
31 255 below section when the structure at the highest compression deformation Figure 9(a). However, at
32 256 period 0.86 s, the pressure on top section becomes higher than the lower section. Figure 10 shows
33 257 velocity profile of marrow during gait loading cycle at different time frame. As can be seen, at period
34 258 0.14s, the velocity was higher than at period 0.86 s. The velocity was range of 0.09 $\mu\text{m/s}$ to 81.2 $\mu\text{m/s}$
35 259 at period of 0.14 s and 0.001 $\mu\text{m/s}$ to 2.6 $\mu\text{m/s}$ at period 0.86 s.
36
37 260

38 261

39 262
40 263 **Figure 8:** Maximum shear stress and pressure distribution on the trabecular bone along with normal
41 264 walking loading
42
43 265

44 266

45
46 267 **Figure 9:** Comparison of pressure distribution on the trabecular bone cross section at different time
47 268 frame (a) $t = 0.14$ s and (b) $t = 0.86$ s
48

49 269

50 270 **Figure 10:** Velocity profile on the trabecular bone at different time frame (a) $t = 0.14$ s and (b) $t = 0.86$
51 271 s during normal gait loading.
52
53 272

54 273

55 274 Multiple regression analysis for morphological parameters is tabulated in Table 2 and Table 3 with
56 275 Pearson correlation and p -value for solid and fluid characteristic. Bone volume fraction and SMI shows
57 276 good correlation with principal strain and von Mises stress. However, the SMI value only significant
58 277 with principal strain and bone volume fraction solitary shows significant value with von Mises stress.
59
60 278

1
2
3 273 As for marrow characteristic, velocity and pressure were significant to SMI, while shear stress is
4 274 insignificant with all morphological parameters.

5
6 275

7
8 276 **Table 2:** Morphological parameters of trabecular bone sample with Pearson correlation and p -value in
9 277 relation with mechanical behaviour.

10
11 278

12
13 279 **Table 3:** Morphological parameters of trabecular bone sample with Pearson correlation and p -value in
14 280 relation with fluid characteristics.

15
16 281

17 282 The volume fraction plays a major role in trabecular bone mechanical properties. The distribution of
18 283 von Mises stress on different model with different bone volume fraction is shown in Figure 11. As can
19 284 be seen, low bone volume fraction model result in higher von Mises stress compare with a model which
20 285 has high volume fraction.

21
22 286

23
24 287 **Figure 11:** Comparison of von Mises stress on the trabecular bone with different bone fraction (a)
25 288 BV/TV = 0.32 and (b) BV/TV = 0.45

26
27 289

28 290 **Figure 12:** Linear relationship between (a) BV/TV and (b) SMI with permeability

29
30 291

31 292 The permeability and trabecular stiffness relationship to bone volume fraction and SMI are plotted in
32 293 Figure 12. The graph showed a strong and negative correlation between the permeability and bone
33 294 volume fraction ($r = -0.862$), whereas the correlations are strong and positive between permeability and
34 295 SMI ($r = 0.835$). Meanwhile, in Figure 13 shows both bone volume fraction and SMI have a strong
35 296 correlation with the trabecular stiffness ($r = 0.832$ and $r = -0.796$; respectively). However, the trabecular
36 297 bone stiffness correlation was inversely compared to the permeability.

37
38 298

39 299 **Figure 13:** Linear relationship between (a) BV/TV and (b) SMI with stiffness.

40
41 300

42 301 **4.0 DISCUSSION**

43
44 302

45 303 The trabecular bone structure is known as a porous structure which contributes to maximum strength
46 304 while giving the bone less weight. Understanding the bone marrow flow and trabecular bone structure
47 305 mechanism can provide insight into bone remodelling process and bone strength. It is vital to identify
48 306 which architectural features that affect the trabecular strength. Thus, in this study, finite element
49 307 analysis with FSI approach was used to identify the architecture contribution with the presence of bone
50 308 marrow when there is physical loading involved.

51
52 309

1
2
3 309 During physiological activities, the bone will have a deformation due to the mechanical load (3). The
4 310 compressive and tensile stress is generated in the trabecular structure which causes the bone marrow
5 311 within the structure to drift from region of compression to tension. Due to the complex structure of
6 312 trabecular bone with small rods, plated and pores, there will be shear stress generated on the wall
7 313 structure. Bone marrow function in activating the bone cells to start the bone remodelling process. Thus,
8 314 this study analysed shear stress, pressure, and permeability to identify the fluid characteristic through
9 315 physical activity. Moreover, the trabecular bone architecture and volume fraction play an important role
10 316 in its mechanical properties. In addition, this study analysed the bone marrow permeability and
11 317 trabecular stiffness with correlation to the trabecular morphology. Applied physiological gait loading
12 318 in this present study to assure more reliable and safer prediction of bone marrow behaviour and
13 319 trabecular stiffness.

20 320
21 321 In the analysis, it can be seen that the maximum peak von Mises stress range for all ten models are 91
22 322 kN/m² to 114 kN/m². The maximum value was identified in period 0.14s, which is due to the fact that
23 323 higher contact force occurs at that period of time (Figure 7). Assessing the von Mises stress in the
24 324 trabecular model was necessary with purpose of providing new insight in prediction of trabecular
25 325 structure failure and evaluating the fracture risk. The permeability in this study was also in agreement
26 326 with results from the literature.

27 327
28 328 The aim of this study is to identify the bone marrow movement behaviour within the trabecular structure
29 329 sufficient for bone cell growth based on physiological activity. Normal walking loading was chosen
30 330 since it is reported as the most frequent physiological activity (26). The results show that during normal
31 331 walking loading, the maximum shear stress occurs is all models are in range 0.05 Pa to 0.27 Pa.
32 332 Furthermore, Li et al. (17), Castillo and Jacobs (20) present that the shear stress was needed for the cells
33 333 to differentiate and proliferate. Moreover, the previous experimental study showed that shear stress in
34 334 the range of 0.1 Pa to 1 Pa needed to stimulate bone cells in vitro. Thus, a much lower range of shear
35 335 stress is suggested to simulate the stress on bone cells during normal walking. However, other
36 336 previously study mention that 0.23 Pa of shear stress is sufficient for regulated bone cells to respond
37 337 and synthesise bone matrix protein for bone remodelling process (33). Additionally, there is separate
38 338 study by Nauman et al. (34) stated that the bone cells stimulation is unaffected by difference shear stress
39 339 levels.

40 340
41 341 Walking 10000 step per day has been proposed as daily activity for healthy adults. This
42 342 recommendation was studied, and it is found that 10000 step per day can improve individual's health
43 343 and sustainability. For example, previous studies stated higher step count per day could lower the
44 344 prevalence of depression (35). In addition, it is observed the Body Mass Index (BMI) of the group with
45 345 higher step count per day has shown significantly lower compared with another group (36).

1
2
3 346 Nevertheless, there is no studies indicate on bone health based on daily step count. However, based on
4 347 the results of this study, it is suggested that higher step count will lead to more shear stress. Thus, can
5 348 help in improving the bone remodelling process and bone strength.
6
7

8 349

9 350 Moreover, while the trabecular bone deforms according to the physiological load, there would be
10 351 pressure difference within the structure (Figure 8). Previous study stated bone formation increase with
11 352 pressure. Welch et al. (37) in their study found that bone marrow pressure increased about 2000 Pa
12 353 resulted in bone remodelling. Another study on the new bone formation of mouse tibiae, stated in
13 354 dynamic compression induced a similar range of pressure value (38). This study results for pressure
14 355 distribution in normal walking gait loading for all models was in the range of 180 Pa to 4000 Pa.
15 356 Addition to this study result analysis, it is found that higher bone volume fraction will lead to lower
16 357 pressure value (Table 3). However, the pressure difference also depends on a variety of factors,
17 358 including the bone marrow rheology, bone strain and permeability (39, 40).
18
19

20 359

21 360 In addition, the results show that the pressure gradient along the walking gait loading was different at
22 361 period 0.14s and 0.86 s as in Figure 9. This is where the bone marrow function as hydraulic stiffening
23 362 effect. Hydraulic stiffening effect refers to the reduction of bone stress during dynamic loading effect
24 363 by the presence of fluid within the structure (41). While at period 0.14s is when the maximum
25 364 compression occurs, the pressure of bone marrow was high at the bottom. This pressure might support
26 365 a certain amount of applied load which caused the apparent stiffness to the trabecular structure.
27 366 Similarly, at period of 0.86s, where tensile occur, the pressure was high at the upper region giving the
28 367 structure extra load barrier which prevents the structure to have high deformation.
29
30

31 368

32 369 This study used BoneJ plugin in the ImageJ software to analyse the morphological data of the trabecular
33 370 model. In the correlation study, only bone volume fraction (BV/TV) and SMI shows a significant value
34 371 with the simulation results. Thus, this study correlated the permeability and bone stiffness with these
35 372 both morphological parameters. From the results, permeability and stiffness show good correlation
36 373 with the BV/TV. Permeability in trabecular bone was vital since it demonstrated the biological based
37 374 features of trabecular bone. Still, the simulation results were consistent to those found in the previous
38 375 literature (42). Additionally, the trabecular bone mechanical quality was depending on its stiffness,
39 376 since the stiffness have a strong correlation with the strength (43).
40
41

42 377

43 378 Hypothetically bone with lower bone volume fraction means porous structure (osteoporotic bone).
44 379 Thus, as mention by Goldstein et al. (44) and Syahrom et al. (45), the trabecular bone integrity and bone
45 380 marrow permeability can be disarrange based on the porosity value. In addition, the results of this study
46 381 suggests that enhancement of bone remodelling process can be achieved by optimization of BV/TV and
47 382 permeability value. However, from the results analysis the reduction of BV/TV can cause higher stress
48
49
50
51
52
53
54
55
56
57
58
59
60

1
2
3 383 on the trabecular structure (Figure 11) and the loss of trabecular structure stiffening effect (Figure 13).
4 384 Therefore, important to find the optimum bone volume fraction which has a good stiffening value and
5 385 yet able to deliver sufficient nutrient to bone cells.
6
7

8 386
9 387 Other than bone volume fraction, the SMI also shows high correlation with the stiffness. The SMI is a
10 388 measurement which determines a porous structure is made of rod or plate-like structure. The value
11 389 starts from 0 for ideal plate structures to 3 for ideal rod structure (46). Theoretically, the plate-like
12 390 structure could barricade more fluid flow compared to the rod-like structure. In contrast with the
13 391 permeability, the stiffness is negatively correlated with the SMI. Moreover, previous study already
14 392 stated that trabecular plates have more dominant role in mechanical integrity of trabecular bone
15 393 structure (47, 48). Also, osteoporotic trabecular bone has been found to have an apparent transition of
16 394 microarchitecture, which is from plate like to rod-like structure (47). Stein et al. (49) in their study
17 395 found that the bone stiffness related with trabecular connectivity, trabeculae orientation and trabecular
18 396 plates. Thus, in correspondence to previous studies, our results suggest that plate-like trabecular
19 397 structure (lower SMI value) can contribute to higher trabecular stiffness.
20
21
22
23
24
25
26

27 398
28 399 There are a few limitations in the interpretation of results that should be considered. This study has
29 400 employed trabecular samples from anatomic site of bovine femoral bone. As such, the microarchitecture
30 401 parameters may differ from that of the human bone or other anatomic sites. However, there are a few
31 402 works done that demonstrate agreement between the architecture as well as mechanical properties of
32 403 bovine trabecular bone and that of a healthy human (50, 51). Furthermore, the impact of marrow phase
33 404 on the trabecular structure can be further investigated in terms of its properties such as the variation of
34 405 constituents and viscosity.
35
36
37
38
39

40 406
41 407 In summary, this study was investigated on the correlation of the morphology parameters onto the
42 408 mechanical properties of trabecular bone with presence of bone marrow. The bone volume fraction and
43 409 SMI were identified as the one that has a higher correlation with the trabecular permeability and
44 410 stiffness compared with others morphological parameters. Moreover, the bone marrow behaviour
45 411 through the physiological activity was identified in this study. This study provides insight into
46 412 understanding how human daily physiological activities contribute to the bone remodelling process and
47 413 nutrient transport with the bone environment. However, more knowledge in this area was crucial to
48 414 studying the bone adaption to the bone replacement and in estimating fracture risk.
49
50
51
52
53

54 415 **5.0 CONCLUSION**

55 416
56 417 The overall aim of this study was to assess the importance on the interaction between the bone marrow
57 418 and trabecular bone structure during mechanical loading by using the FSI approach. Trabecular bone

1
2
3 419 is known as a highly porous structure with a significant volume of bone marrow, a compressive or
4 420 tensile force on the trabecular bone will result in bone marrow movement with respect to the trabecular
5 421 bone structure. It is believed that the fluid flow will cause the shear stress to the trabecular structure.
6 422 The interaction between the fluid and trabecular bone will occur, and this incident might have several
7 423 effects on the trabecular structure. Moreover, bone remodelling process was occurring due to the shear
8 424 stress on the bone cell which triggers the process. In addition to shear stress, based on previous study
9 425 the hydraulic stiffening effect occurs due to the presence of bone marrow within the trabecular bone
10 426 structure. Therefore, this study proposed the used of FSI approach to model the trabecular bone
11 427 behaviour and marrow flow characteristic.

12 428 The physiological activities in daily human life play a major role than calcium intake in the bone
13 429 development process (52). It contributes to mechanical stimuli in bone marrow and trabecular bone
14 430 strain. Normal walking is one of human major daily activity is chosen in this study as a boundary
15 431 condition in analysing the trabecular bone behaviour. The bone marrow behaviour was recorded during
16 432 the normal walking cyclic loading. While the trabecular bone deforms according to the physiological
17 433 load, the bone marrow within will encounter mechanical stimulation in mechanobiological response
18 434 (53, 54). The shear stress value along normal walking gait loading was found in a range of 0.05 to 0.27
19 435 Pa which is sufficient to regulate cell response minimally (33). However, due to ageing factor, bone
20 436 resorption rate will become higher. Thus, higher shear stress was needed in order to have rapid bone
21 437 remodelling process to encounter the bone resorption rate. Furthermore, this study also provides insight
22 438 into understanding the related mechanobiological of bone cells and disease in deterioration of nutrient
23 439 supplied to the bone.

24 440

25 441 **Acknowledgments**

26 442 This project was sponsored by the Universiti Teknologi Malaysia (UTM) and Universitas Airlangga
27 443 (Unair) through the Grant scheme (R.J130000.7309.4B535) matching grant scheme. The authors would
28 444 also like to thank the Research Management Centre, Universiti Teknologi Malaysia, for managing the
29 445 project.

30 446

31 447 **6.0 References**

- 32 448 1. Saad APM, Syahrom A. Study of dynamic degradation behaviour of porous magnesium
33 449 under physiological environment of human cancellous bone. *Corrosion Science*. 2018;131:45-
34 450 56.
- 35 451 2. Yourek G, McCormick SM, Mao JJ, Reilly GC. Shear stress induces osteogenic
36 452 differentiation of human mesenchymal stem cells. *Regenerative medicine*. 2010;5(5):713-24.

- 1
2
3 453 3. Coughlin TR, Niebur GL. Fluid shear stress in trabecular bone marrow due to low-
4 454 magnitude high-frequency vibration. *Journal of biomechanics*. 2012;45(13):2222-9.
- 5 455 4. Vaughan T, Voisin M, Niebur G, McNamara L. Multiscale modeling of trabecular bone
6 456 marrow: understanding the micromechanical environment of mesenchymal stem cells during
7 457 osteoporosis. *Journal of Biomechanical Engineering*. 2015;137(1).
- 8 458 5. You L, Cowin SC, Schaffler MB, Weinbaum S. A model for strain amplification in the
9 459 actin cytoskeleton of osteocytes due to fluid drag on pericellular matrix. *Journal of*
10 460 *biomechanics*. 2001;34(11):1375-86.
- 11 461 6. Adachi T, Kameo Y, Hojo M. Trabecular bone remodelling simulation considering
12 462 osteocytic response to fluid-induced shear stress. *Philosophical Transactions of the Royal*
13 463 *Society A: Mathematical, Physical and Engineering Sciences*. 2010;368(1920):2669-82.
- 14 464 7. Wittkowske C, Reilly GC, Lacroix D, Perrault CM. In vitro bone cell models: impact
15 465 of fluid shear stress on bone formation. *Frontiers in Bioengineering and Biotechnology*.
16 466 2016;4:87.
- 17 467 8. Birmingham E, Niebur G, McNamara L, McHugh P. An experimental and
18 468 computational investigation of bone formation in mechanically loaded trabecular bone
19 469 explants. *Annals of biomedical engineering*. 2016;44(4):1191-203.
- 20 470 9. Shen V, Liang X, Birchman R, Wu D, Healy D, Lindsay R, et al. Short term
21 471 immobilization-induced cancellous bone loss is limited to regions undergoing high turnover
22 472 and/or modeling in mature rats. *Bone*. 1997;21(1):71-8.
- 23 473 10. Rodriguez N, Herndon D, Klein G. Evidence against a role of immobilization in the
24 474 bone loss following burns. *Bone*. 2011;2(48):S190.
- 25 475 11. Frost HM. Wolff's Law and bone's structural adaptations to mechanical usage: an
26 476 overview for clinicians. *The Angle Orthodontist*. 1994;64(3):175-88.
- 27 477 12. Frost HM. Bone "mass" and the "mechanostat": a proposal. *The anatomical record*.
28 478 1987;219(1):1-9.
- 29 479 13. Burr DB, Milgrom C, Fyhrie D, Forwood M, Nyska M, Finestone A, et al. In vivo
30 480 measurement of human tibial strains during vigorous activity. *Bone*. 1996;18(5):405-10.
- 31 481 14. Fritton SP, McLeod KJ, Rubin CT. Quantifying the strain history of bone: spatial
32 482 uniformity and self-similarity of low-magnitude strains. *Journal of biomechanics*.
33 483 2000;33(3):317-25.
- 34 484 15. Gurkan UA, Akkus O. The mechanical environment of bone marrow: a review. *Annals*
35 485 *of biomedical engineering*. 2008;36(12):1978-91.
- 36 486 16. McAllister T, Frangos J. Steady and transient fluid shear stress stimulate NO release in
37 487 osteoblasts through distinct biochemical pathways. *Journal of Bone and Mineral Research*.
38 488 1999;14(6):930-6.
- 39 489 17. Li YJ, Batra NN, You L, Meier SC, Coe IA, Yellowley CE, et al. Oscillatory fluid flow
40 490 affects human marrow stromal cell proliferation and differentiation. *Journal of Orthopaedic*
41 491 *Research*. 2004;22(6):1283-9.
- 42 492 18. Knight MN, Hankenson KD. Mesenchymal stem cells in bone regeneration. *Advances*
43 493 *in wound care*. 2013;2(6):306-16.
- 44 494 19. Shao J, Zhang W, Yang T. Using mesenchymal stem cells as a therapy for bone
45 495 regeneration and repairing. *Biological research*. 2015;48(1):62.
- 46 496 20. Castillo AB, Jacobs CR. Mesenchymal stem cell mechanobiology. *Current osteoporosis*
47 497 *reports*. 2010;8(2):98-104.
- 48 498 21. Klein-Nulend J, Van Der Plas A, Semeins CM, Ajubi NE, Erangos JA, Nijweide PJ, et
49 499 al. Sensitivity of osteocytes to biomechanical stress in vitro. *The FASEB Journal*.
50 500 1995;9(5):441-5.

- 1
2
3 501 22. Case N, Sen B, Thomas J, Styner M, Xie Z, Jacobs C, et al. Steady and oscillatory fluid
4 502 flows produce a similar osteogenic phenotype. *Calcified tissue international*. 2011;88(3):189-
5 503 97.
- 6 504 23. Bakker AD, Joldersma M, Klein-Nulend J, Burger EH. Interactive effects of PTH and
7 505 mechanical stress on nitric oxide and PGE2 production by primary mouse osteoblastic cells.
8 506 *American journal of physiology-endocrinology and metabolism*. 2003;285(3):E608-E13.
- 9 507 24. Arnsdorf EJ, Tummala P, Kwon RY, Jacobs CR. Mechanically induced osteogenic
10 508 differentiation—the role of RhoA, ROCKII and cytoskeletal dynamics. *Journal of cell science*.
11 509 2009;122(4):546-53.
- 12 510 25. Yeatts AB, Fisher JP. Bone tissue engineering bioreactors: dynamic culture and the
13 511 influence of shear stress. *Bone*. 2011;48(2):171-81.
- 14 512 26. Bergmann G, Deuretzbacher G, Heller M, Graichen F, Rohlmann A, Strauss J, et al.
15 513 Hip contact forces and gait patterns from routine activities. *Journal of biomechanics*.
16 514 2001;34(7):859-71.
- 17 515 27. Fatihhi S, Harun M, Kadir MRA, Abdullah J, Kamarul T, Öchsner A, et al. Uniaxial
18 516 and multiaxial fatigue life prediction of the trabecular bone based on physiological loading: a
19 517 comparative study. *Annals of biomedical engineering*. 2015;43(10):2487-502.
- 20 518 28. Homminga J, McCreddie BR, Weinans H, Huijskes R. The dependence of the elastic
21 519 properties of osteoporotic cancellous bone on volume fraction and fabric. *Journal of*
22 520 *biomechanics*. 2003;36(10):1461-7.
- 23 521 29. Sylvester AD, Kramer PA. Young's modulus and load complexity: Modeling their
24 522 effects on proximal femur strain. *The Anatomical Record*. 2018;301(7):1189-202.
- 25 523 30. Bayraktar HH, Gupta A, Kwon RY, Papadopoulos P, Keaveny TM. The modified
26 524 super-ellipsoid yield criterion for human trabecular bone. *J Biomech Eng*. 2004;126(6):677-
27 525 84.
- 28 526 31. Bryant J, David T, Gaskell P, King S, Lond G. Rheology of bovine bone marrow.
29 527 *Proceedings of the Institution of Mechanical Engineers, Part H: Journal of Engineering in*
30 528 *Medicine*. 1989;203(2):71-5.
- 31 529 32. Haskill JS, McNeill TA, Moore MAS. Density distribution analysis of In vivo and In
32 530 vitro colony forming cells in bone marrow. *Journal of Cellular Physiology*. 1970;75(2):167-
33 531 79.
- 34 532 33. Kreke MR, Sharp LA, Woo Lee Y, Goldstein AS. Effect of intermittent shear stress on
35 533 mechanotransductive signaling and osteoblastic differentiation of bone marrow stromal cells.
36 534 *Tissue Engineering Part A*. 2008;14(4):529-37.
- 37 535 34. Nauman E, Satcher R, Keaveny T, Halloran B, Bikle D. Osteoblasts respond to pulsatile
38 536 fluid flow with short-term increases in PGE2 but no change in mineralization. *Journal of*
39 537 *Applied Physiology*. 2001;90(5):1849-54.
- 40 538 35. McKercher CM, Schmidt MD, Sanderson KA, Patton GC, Dwyer T, Venn AJ. Physical
41 539 activity and depression in young adults. *American journal of preventive medicine*.
42 540 2009;36(2):161-4.
- 43 541 36. Krumm EM, Dessieux OL, Andrews P, Thompson DL. The relationship between daily
44 542 steps and body composition in postmenopausal women. *Journal of women's health*.
45 543 2006;15(2):202-10.
- 46 544 37. Welch R, Johnston 2nd C, Waldron M, Poteet B. Bone changes associated with
47 545 intraosseous hypertension in the caprine tibia. *JBJS*. 1993;75(1):53-60.
- 48 546 38. Hu M, Cheng J, Qin Y-X. Dynamic hydraulic flow stimulation on mitigation of
49 547 trabecular bone loss in a rat functional disuse model. *Bone*. 2012;51(4):819-25.
- 50 548 39. Teo J, Si-Hoe K, Keh J, Teoh S. Correlation of cancellous bone microarchitectural
51 549 parameters from microCT to CT number and bone mechanical properties. *Materials Science*
52 550 *and Engineering: C*. 2007;27(2):333-9.

- 1
2
3 551 40. Baroud G, Falk R, Crookshank M, Sponagel S, Steffen T. Experimental and theoretical
4 552 investigation of directional permeability of human vertebral cancellous bone for cement
5 553 infiltration. *Journal of biomechanics*. 2004;37(2):189-96.
- 6 554 41. Liebschner MA, Keller TS. Hydraulic strengthening affects the stiffness and strength
7 555 of cortical bone. *Annals of Biomedical Engineering*. 2005;33(1):26-38.
- 8 556 42. Kohles SS, Roberts JB. Linear poroelastic cancellous bone anisotropy: trabecular solid
9 557 elastic and fluid transport properties. *J Biomech Eng*. 2002;124(5):521-6.
- 10 558 43. Lopez KW, Goldstein SA, Ciarelli MJ, Kuhn JL, Brown M, Feldkamp L. The
11 559 relationship between the structural and orthogonal compressive properties of trabecular bone.
12 560 1994.
- 13 561 44. Goldstein AS, Juarez TM, Helmke CD, Gustin MC, Mikos AG. Effect of convection
14 562 on osteoblastic cell growth and function in biodegradable polymer foam scaffolds.
15 563 *Biomaterials*. 2001;22(11):1279-88.
- 16 564 45. Syahrom A, Kadir MRA, Abdullah J, Öchsner A. Permeability studies of artificial and
17 565 natural cancellous bone structures. *Medical engineering & physics*. 2013;35(6):792-9.
- 18 566 46. Hildebrand T, Rüegsegger P. Quantification of bone microarchitecture with the
19 567 structure model index. *Computer Methods in Biomechanics and Bio Medical Engineering*.
20 568 1997;1(1):15-23.
- 21 569 47. Wang J, Zhou B, Liu XS, Fields AJ, Sanyal A, Shi X, et al. Trabecular plates and rods
22 570 determine elastic modulus and yield strength of human trabecular bone. *Bone*. 2015;72:71-80.
- 23 571 48. Wang J, Zhou B, Parkinson I, Thomas CDL, Clement JG, Fazzalari N, et al. Trabecular
24 572 plate loss and deteriorating elastic modulus of femoral trabecular bone in intertrochanteric hip
25 573 fractures. *Bone research*. 2013;1:346-54.
- 26 574 49. Stein EM, Kepley A, Walker M, Nickolas TL, Nishiyama K, Zhou B, et al. Skeletal
27 575 structure in postmenopausal women with osteopenia and fractures is characterized by abnormal
28 576 trabecular plates and cortical thinning. *Journal of Bone and Mineral Research*.
29 577 2014;29(5):1101-9.
- 30 578 50. Keaveny TM, Wachtel EF, Ford CM, Hayes WC. Differences between the tensile and
31 579 compressive strengths of bovine tibial trabecular bone depend on modulus. *Journal of*
32 580 *biomechanics*. 1994;27(9):1137-46.
- 33 581 51. Morgan EF, Yeh OC, Chang WC, Keaveny TM. Nonlinear behavior of trabecular bone
34 582 at small strains. *J Biomech Eng*. 2001;123(1):1-9.
- 35 583 52. Anderson JJ. The important role of physical activity in skeletal development: how
36 584 exercise may counter low calcium intake. *The American journal of clinical nutrition*.
37 585 2000;71(6):1384-6.
- 38 586 53. Metzger TA, Schwaner SA, LaNeve AJ, Kreipke TC, Niebur GL. Pressure and shear
39 587 stress in trabecular bone marrow during whole bone loading. *Journal of biomechanics*.
40 588 2015;48(12):3035-43.
- 41 589 54. Birmingham E, Grogan J, Niebur G, McNamara L, McHugh P. Computational
42 590 modelling of the mechanics of trabecular bone and marrow using fluid structure interaction
43 591 techniques. *Annals of biomedical engineering*. 2013;41(4):814-26.

592

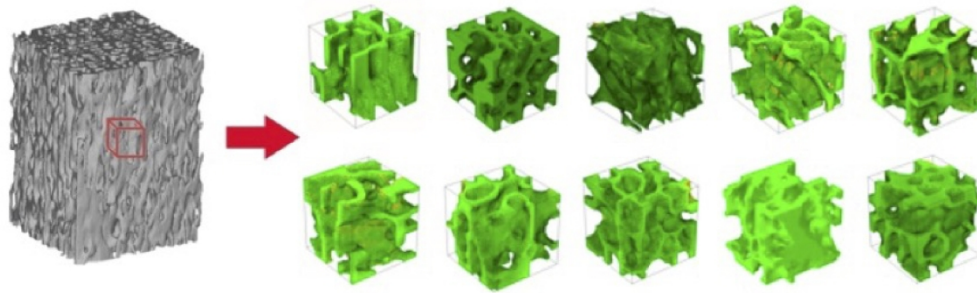


Figure 1: Development of three-dimensional model into sub volume model.

309x95mm (300 x 300 DPI)

1
2
3
4
5
6
7
8
9
10
11
12
13
14
15
16
17
18
19
20
21
22
23
24
25
26
27
28
29
30
31
32
33
34
35
36
37
38
39
40
41
42
43
44
45
46
47
48
49
50
51
52
53
54
55
56
57
58
59
60

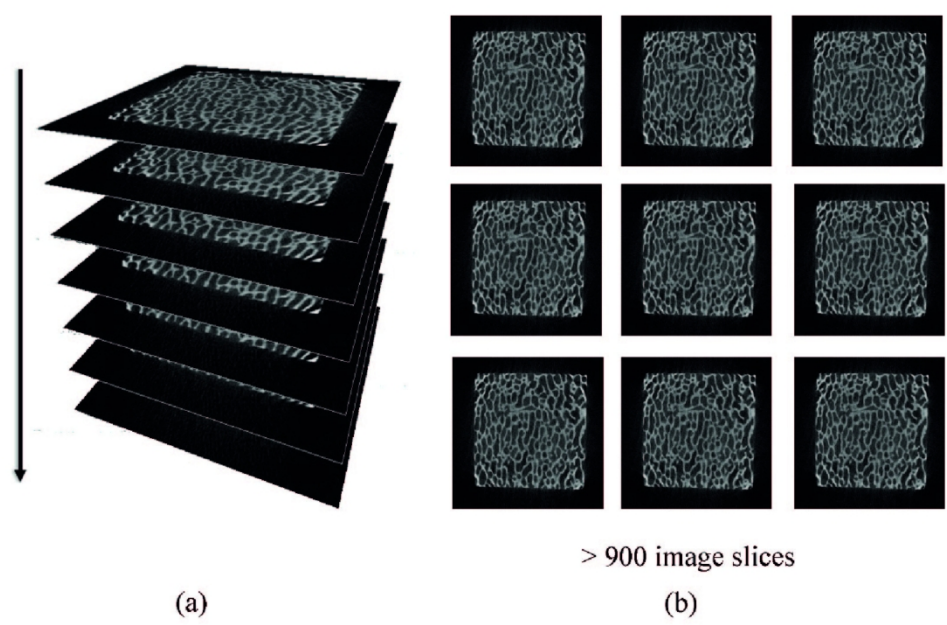


Figure 2: Images obtain from μ -CT scan with (a) Images stacked in sequence according to sample orientation (b) raw scanned images file

145x102mm (300 x 300 DPI)

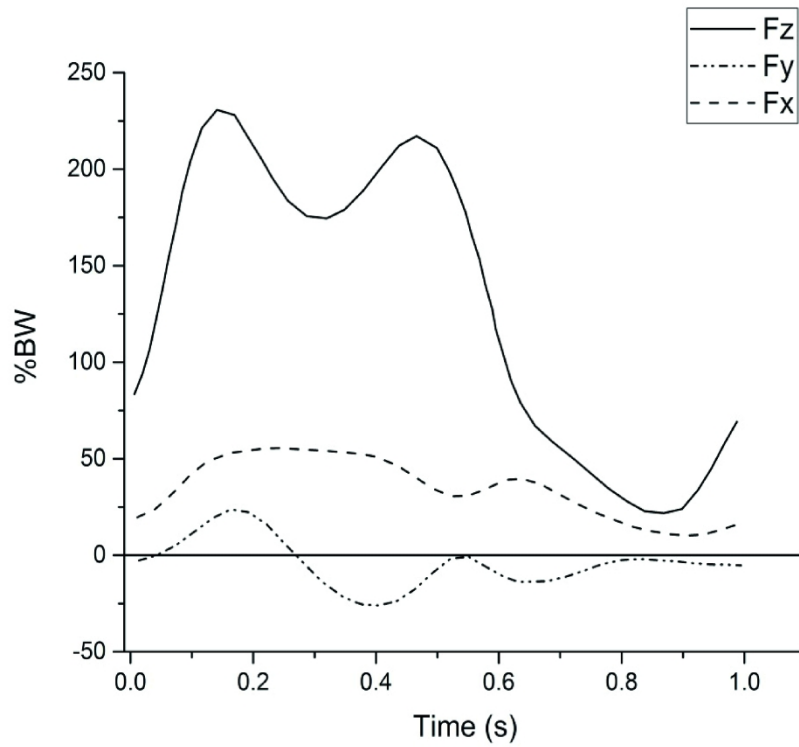


Figure 3: Gait loading of normal walking based on body weight percentage (Bergmann G. et al., 2001).

249x201mm (300 x 300 DPI)

1
2
3
4
5
6
7
8
9
10
11
12
13
14
15
16
17
18
19
20
21
22
23
24
25
26
27
28
29
30
31
32
33
34
35
36
37
38
39
40
41
42
43
44
45
46
47
48
49
50
51
52
53
54
55
56
57
58
59
60

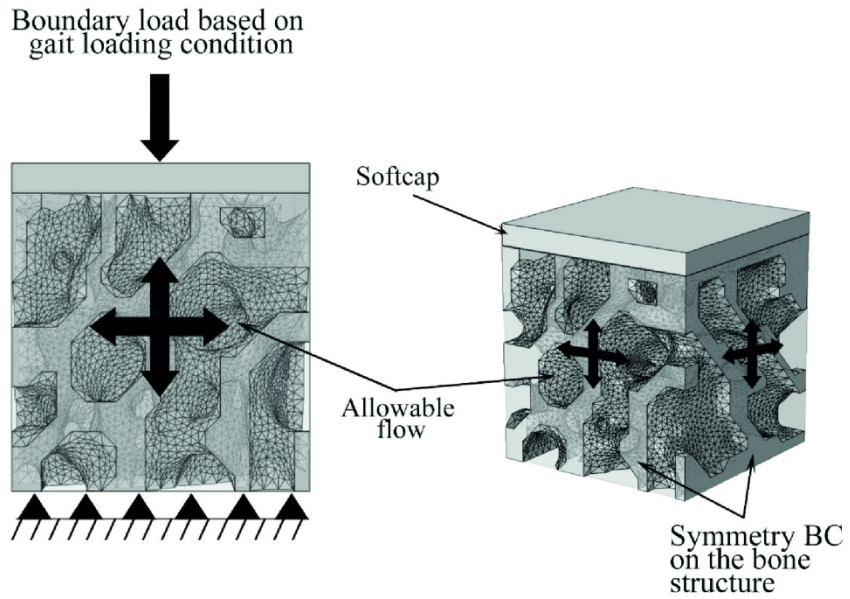


Figure 4 Boundary Conditions (BC) of trabecular bone and bone marrow models

159x98mm (300 x 300 DPI)

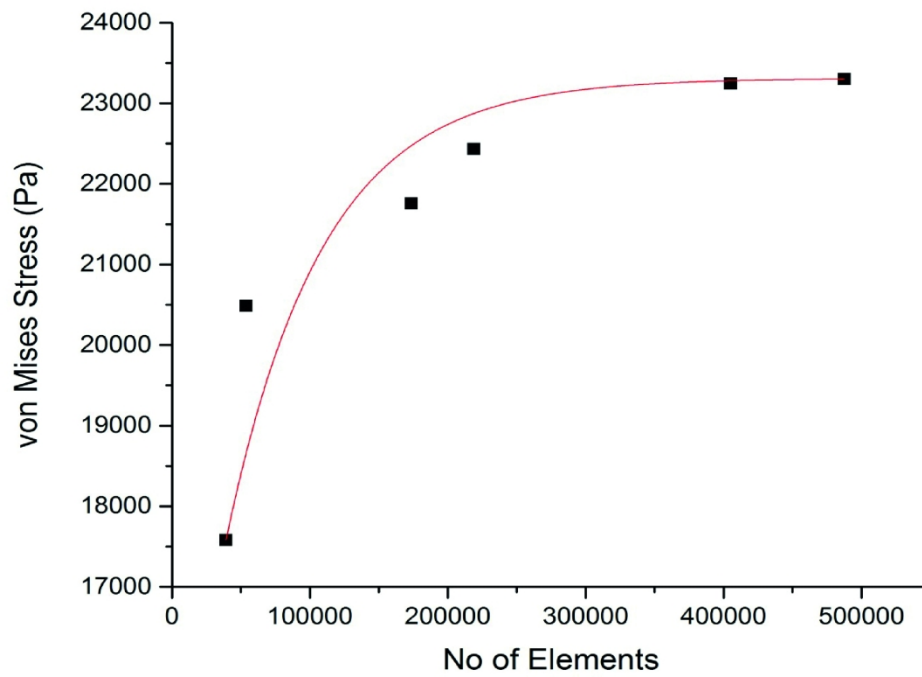


Figure 5 Convergence study for the trabecular structure model

210x147mm (300 x 300 DPI)

1
2
3
4
5
6
7
8
9
10
11
12
13
14
15
16
17
18
19
20
21
22
23
24
25
26
27
28
29
30
31
32
33
34
35
36
37
38
39
40
41
42
43
44
45
46
47
48
49
50
51
52
53
54
55
56
57
58
59
60

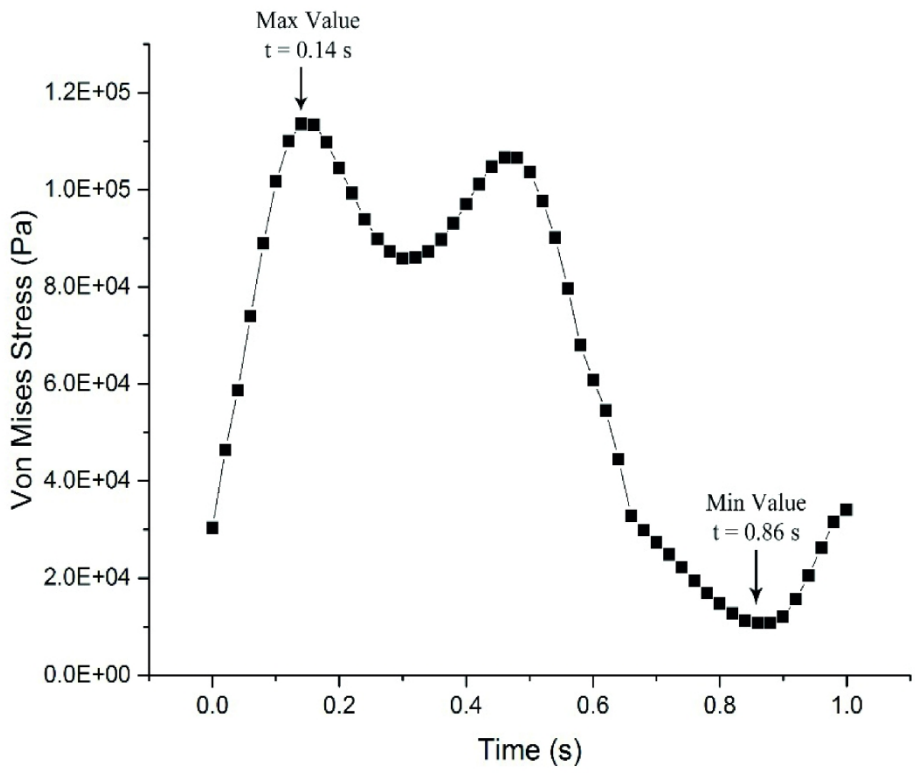
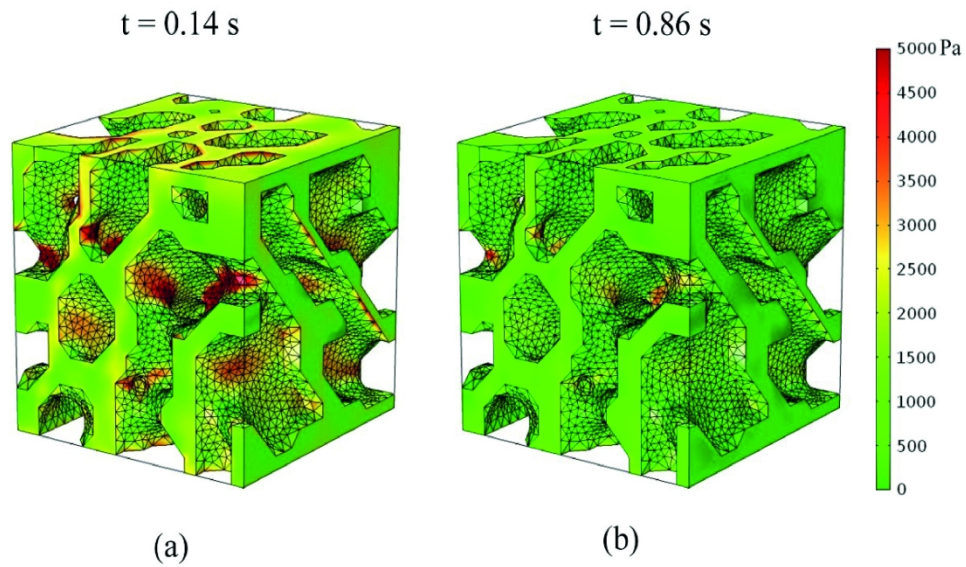


Figure 6: von Mises stress distribution on the trabecular bone during normal walking

210x169mm (300 x 300 DPI)



27
28
29
30
31
32
33
34
35
36
37
38
39
40
41
42
43
44
45
46
47
48
49
50
51
52
53
54
55
56
57
58
59
60

Figure 7: Comparison of von Mises stress on the trabecular bone at different time frame (a) $t = 0.14$ s and (b) $t = 0.86$ s

210x134mm (300 x 300 DPI)

1
2
3
4
5
6
7
8
9
10
11
12
13
14
15
16
17
18
19
20
21
22
23
24
25
26
27
28
29
30
31
32
33
34
35
36
37
38
39
40
41
42
43
44
45
46
47
48
49
50
51
52
53
54
55
56
57
58
59
60

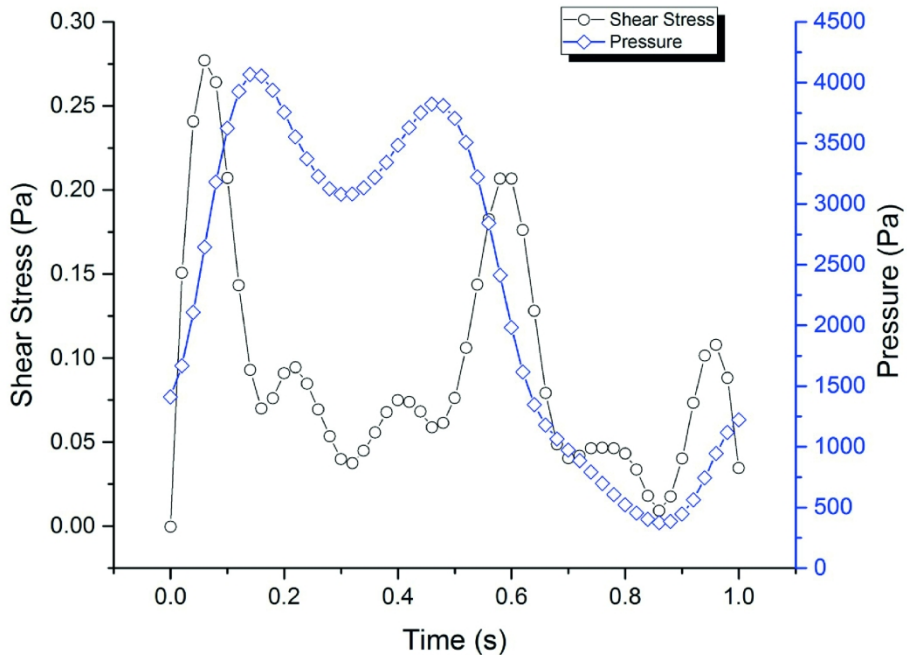


Figure 8: Maximum shear stress and pressure distribution on the trabecular bone along with normal walking loading

210x159mm (300 x 300 DPI)

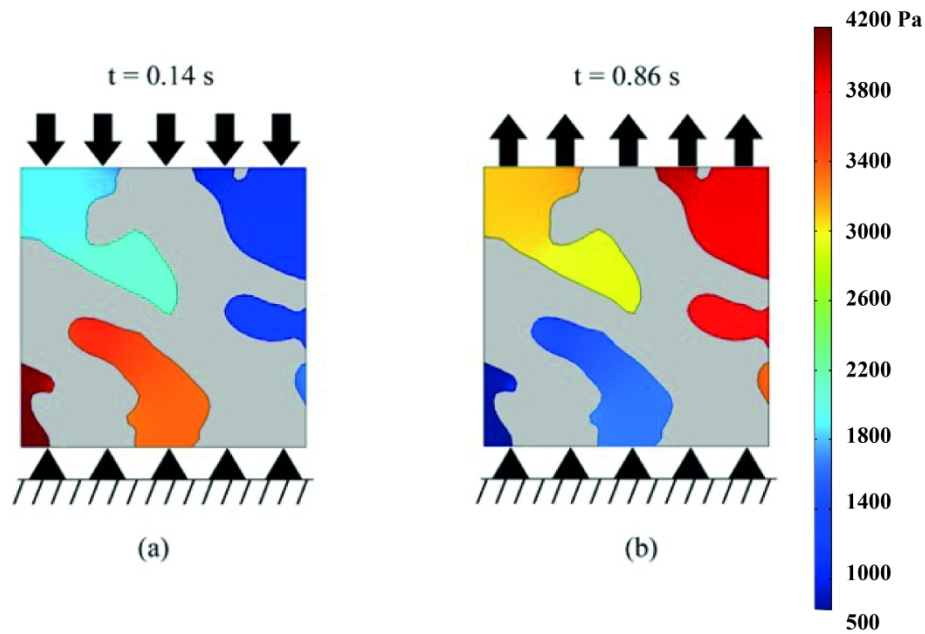


Figure 9: Comparison of pressure distribution on the trabecular bone cross section at different time frame
(a) $t = 0.14$ s and (b) $t = 0.86$ s

308x220mm (300 x 300 DPI)

1
2
3
4
5
6
7
8
9
10
11
12
13
14
15
16
17
18
19
20
21
22
23
24
25
26
27
28
29
30
31
32
33
34
35
36
37
38
39
40
41
42
43
44
45
46
47
48
49
50
51
52
53
54
55
56
57
58
59
60

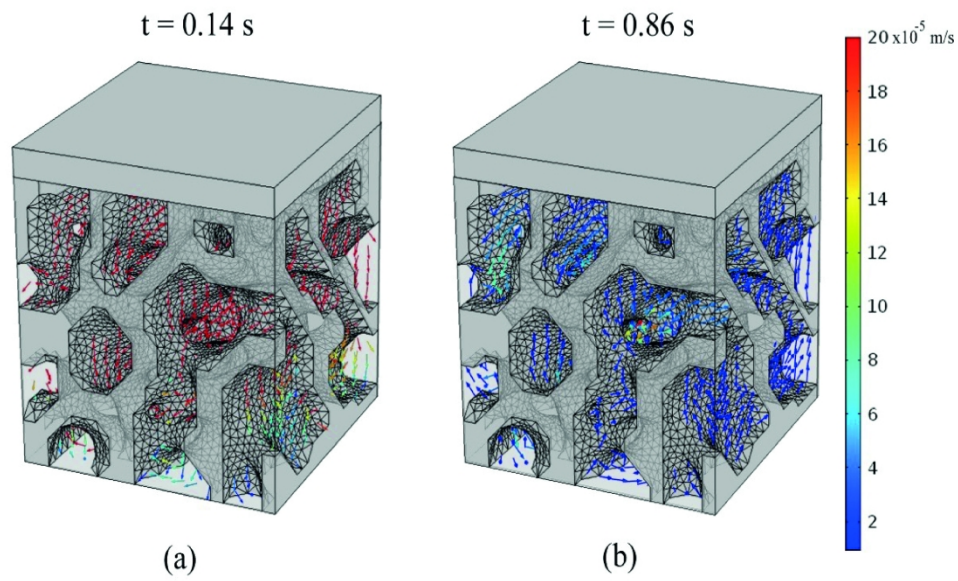


Figure 10: Velocity profile on the trabecular bone at different time frame (a) $t = 0.14 \text{ s}$ and (b) $t = 0.86 \text{ s}$ during normal gait loading.

292x184mm (300 x 300 DPI)

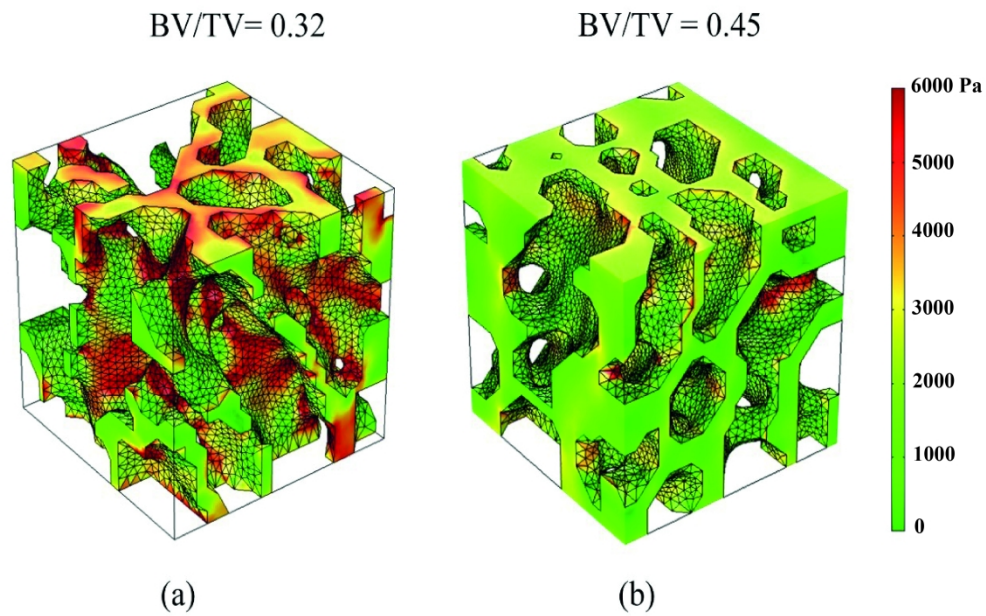


Figure 11: Comparison of von Mises stress on the trabecular bone with different bone fraction (a) BV/TV = 0.32 and (b) BV/TV = 0.45

298x212mm (300 x 300 DPI)

1
2
3
4
5
6
7
8
9
10
11
12
13
14
15
16
17
18
19
20
21
22
23
24
25
26
27
28
29
30
31
32
33
34
35
36
37
38
39
40
41
42
43
44
45
46
47
48
49
50
51
52
53
54
55
56
57
58
59
60

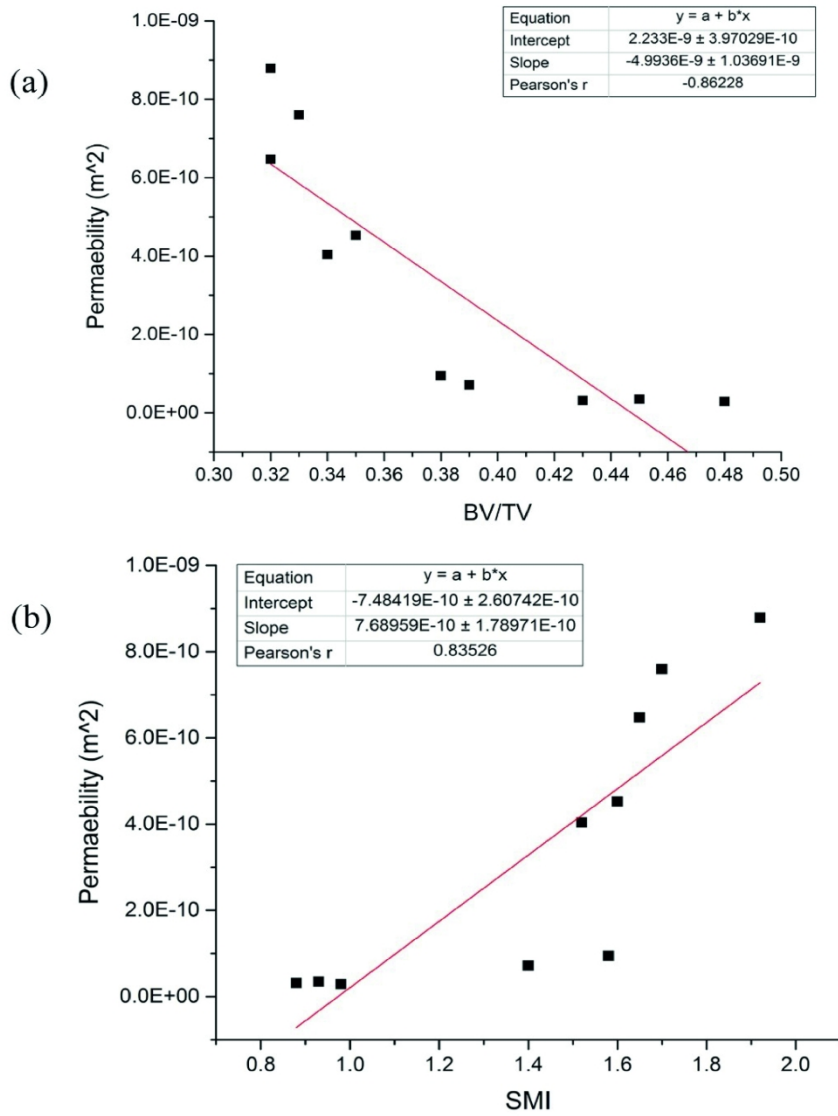


Figure 12: Linear relationship between (a) BV/TV and (b) SMI with permeability

209x241mm (300 x 300 DPI)

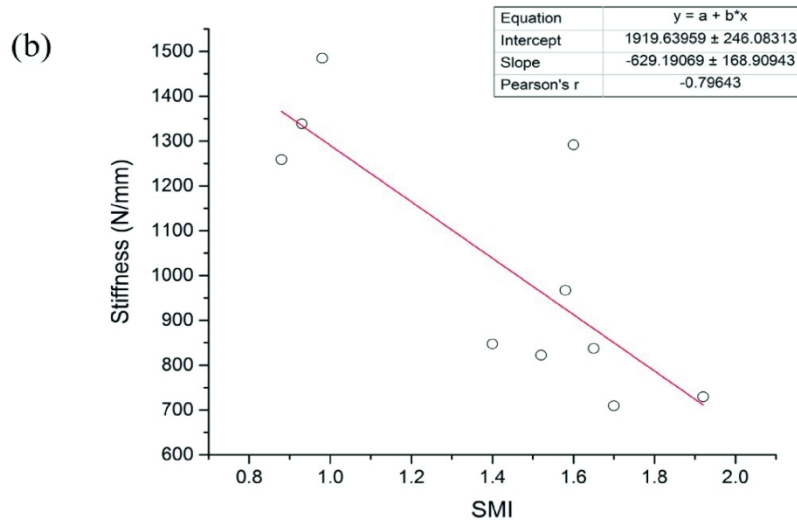
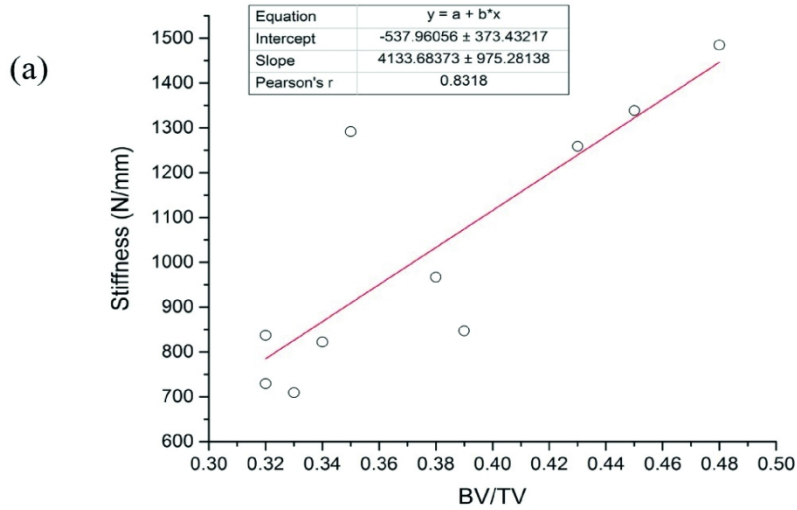


Figure 13: Linear relationship between (a) BV/TV and (b) SMI with stiffness.

209x238mm (300 x 300 DPI)

Table 1: Morphological indices of trabecular bone sample

PARAMETER	MINIMUM	MAXIMUM	MEAN	SD
BV/TV	0.318	0.477	0.379	0.057
Tb.Th (mm)	0.128	0.559	0.207	0.057
Tb.Sp (mm)	0.253	1.022	0.441	0.137
BS/BV	11.313	15.857	13.677	1.719
DA	0.38	0.684	0.611	0.146
Conn.D (mm ⁻³)	19.625	59.875	37.975	14.179
SMI	0.875	1.918	1.416	0.316
Porosity (%)	62	76	70	5
Bone Surface Area (mm ²)	28.802	37.518	32.447	3.134

Table 2: Morphological parameters of trabecular bone sample with Pearson correlation and p -value in relation with mechanical behaviour.

Morphological Parameters	Principle Strain		Von Mises Stress	
	Pearson Correlation	p -value	Pearson Correlation	p -value
BV/TV	-0.830	0.123	-0.798	0.006*
BS/TV	0.449	0.452	0.28	0.132
SMI	0.850	0.002*	0.715	0.689
Conn. D	-0.032	0.916	-0.303	0.16
Tb.Th	-0.426	0.566	-0.344	0.206
Tb.Sp	0.705	0.403	0.769	0.405
DA	0.410	0.966	0.559	0.218

*Significant p -value < 0.05

Table 3: Morphological parameters of trabecular bone sample with Pearson correlation and p -value in relation with fluid characteristics.

Morphology Parameters	Velocity		Pressure		Shear Stress	
	Pearson Correlation	p -value	Pearson Correlation	p -value	Pearson Correlation	p -value
BV/TV	-0.661	0.969	-0.672	0.168	0.001	0.499
BS/TV	0.388	0.449	0.53	0.585	0.411	0.119
SMI	0.710	0.022*	0.825	0.003*	0.029	0.469
Conn. D	-0.049	0.316	0.288	0.815	0.184	0.306
Tb.Th	-0.296	0.395	-0.346	0.209	-0.424	0.111
Tb.Sp	0.607	0.735	0.594	0.754	-0.255	0.239
DA	0.324	0.468	0.074	0.721	0.079	0.414

*Significant p -value < 0.05

Reviewer(s)' Comments to Author:

Reviewer: 1

Comments to the Author

The paper presents an interesting analysis on the effect of bone marrow on the mechanical environment and the structure of trabecular bone during normal walking loading.

However, there are comments and questions that need to be addressed.

1. Abstract – “FSI approach”, define the meaning of FSI.
→ Definition added.
2. Line 72 – Units of micro-strain ($\mu\epsilon$) are somehow different from what is used on mechanical engineering. Could it be replaced by mm/mm?
→ Replaced accordingly.
3. Line 83 – Define MSCs
→ Definition added.
4. Line 116 – the protocol for storage and cleaning was previously defined? If so, give a reference.
→ Reference added.
5. Table 1 –If possible, also add Tb.N (trabecular number) and FD (fractal dimension)
→ We decided not to include Tb.N and FD on the table as both indices do not directly related to the focus of this study.
6. Line 177 – Figure Caption – Was this figure obtained under the present work or does it belong to another author?
→ Yes, it is belonged to another author. Citation added.
7. Line 175 – The authors should add in the text that the convergence study was performed with the criterion of the von Mises stress variation less than X %. Usual values are 2 to 5%. What was the value here?
→ The variation was less than 5% of the von Mises stress criterion.
Explanation added on line 177 – “The analysis was performed with the criterion of the von Mises stress criterion less than 5%.”
8. Line 196, page 11, provide a number of each equation.
→ Numbers added to all equations.
9. Line 215 “.....With n is the normal acting outward at the boundary,...” needs an English revision
→ Sentence was revised accordingly – “With the normal, n is acting outward from surface boundary,...”

10. Line 250 – add in the caption that the time chosen corresponds to the highest and to the lowest von Mises stress.
→ Added accordingly.
11. Line 271 – Could the authors add a scale of colors at Figure 9?
→ Added accordingly.
12. Line 306 – The number of the figure is missing, but it should be 12.
→ Added accordingly.
13. Line 308, also the number of the figure is missing.
→ Added accordingly.
14. Line 400 and 401 – Figures number is missing
→ Added accordingly.

Reviewer: 2

Comments to the Author

The language used needs reviewing by a native English reader.

→ Done, the manuscript was send for proofread.

The temperatures used are confusing, for example “frozen at -18°C to 26°C ”, or “below 46°C ”

→ revised accordingly.

There were 10 models generated and tested in this study. Can the models be shown ?

→ Added accordingly. Please refer figure 1

Density is wrong: “Newtonian fluid with density of 1.06 kg/m^3 ”
→ Thank you very much, you are correct we wrong give a unit supposly (g/cm^3). We are update become 1060 Kg/m^3 , Please refer line 193

S is not the Piola-Kirchhoff stress

→ Revised into second Piola-Kirchhoff stress.

What was the load applied to the model ?

→ Load applied based on gait loading condition (Please refer figure 3)

In relation to the Fluid boundary conditions, marrow cannot enter or exit your model, is this correct ?

→ The fluid boundary condition was used allowable flow, then the fluid region can enter and or exit the model.

What software was used for the FSI simulations ?

→ COMSOL Multiphysics.

No details are given for the Eulerian mesh

→ Please refer line 175-182 and convergence study figure 5.

What about accelerations and inertial effects? walking is a dynamical event, and it is common sense that this would have influence on the results.

→ In this study researcher not consider acceleration and inertial effect.

However gait loading was used as load in boundary condition. we have agree acceleration and inertial effect may have influence on the result and we will consider for next study. Thank you for your suggestion.

--